Sphingosine Kinase-2 Inhibition Promotes Immunogenic Differentiation of Myeloid-Derived Suppressor Cells through an Acetyl-CoA Carboxylase-Phosphatidylcholine Axis

Paramita Chakraborty[1], Shikhar Mehrotra[1*]

[1]Departments of Pharmacology & Immunology, Hollings Cancer Center, Medical University of South Carolina, Charleston, South Carolina, USA.

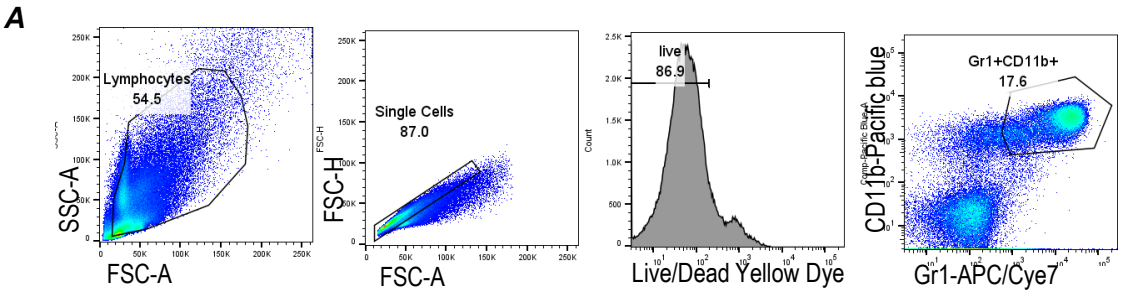
A
Lymphocytes
54.5
SSC-A
FSC-A
Single Cells
87.0
FSC-H
FSC-A
live
86.9
Count
Live/Dead Yellow Dye
Gr1+CD11b+
17.6
CD11b-Pacific blue
Gr1-APC/Cye7

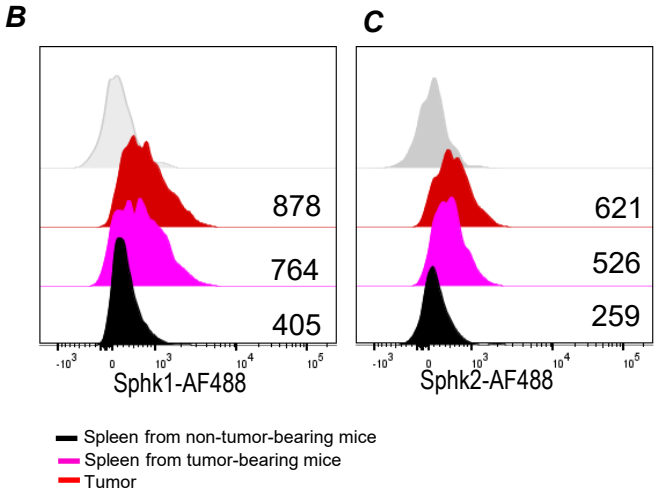
B
878
764
405
Sphk1-AF488
C
621
526
259
Sphk2-AF488
Spleen from non-tumor-bearing mice
Spleen from tumor-bearing mice
Tumor

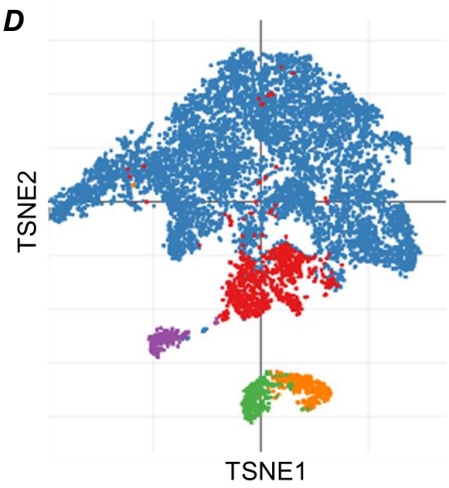
D
TSNE2
TSNE1

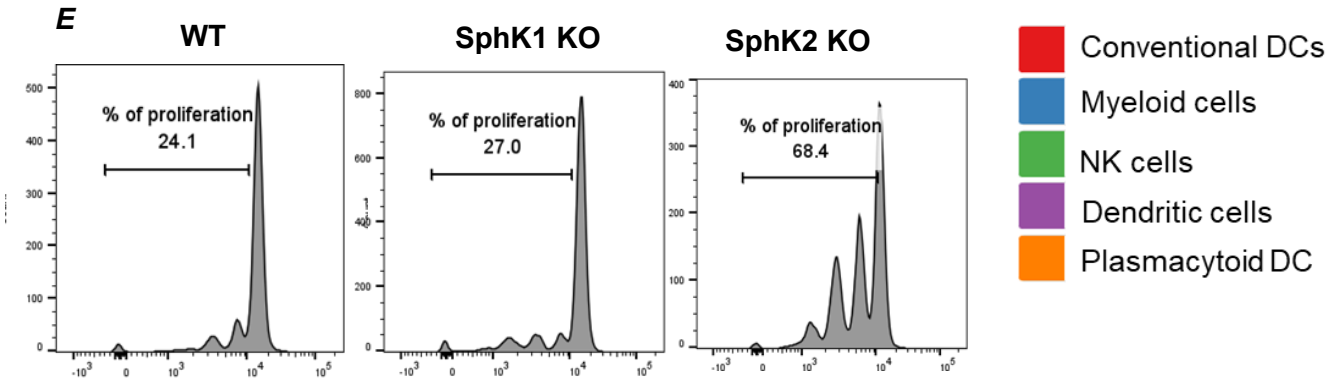
E
WT
% of proliferation
24.1
SphK1 KO
% of proliferation
27.0
SphK2 KO
% of proliferation
68.4
Conventional DCs
Myeloid cells
NK cells
Dendritic cells
Plasmacytoid DC

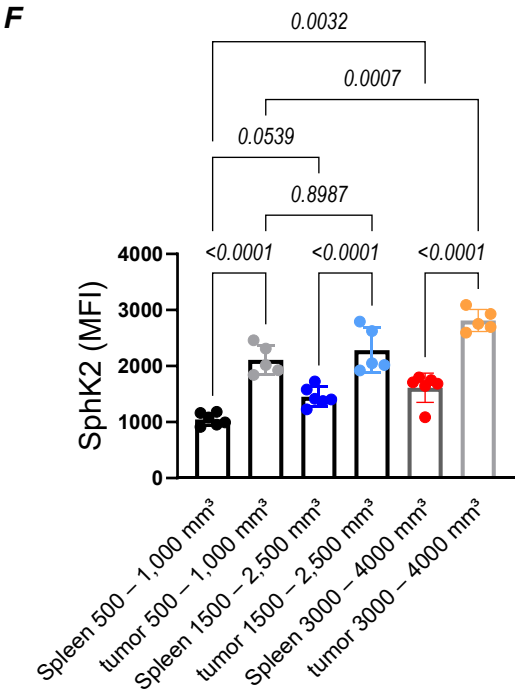
F
0.0032
0.0007
0.0539
0.8987
<0.0001
<0.0001
<0.0001
SphK2 (MFI)
Spleen 500 – 1,000 mm³
tumor 500 – 1,000 mm³
Spleen 1500 – 2,500 mm³
tumor 1500 – 2,500 mm³
Spleen 3000 – 4000 mm³
tumor 3000 – 4000 mm³

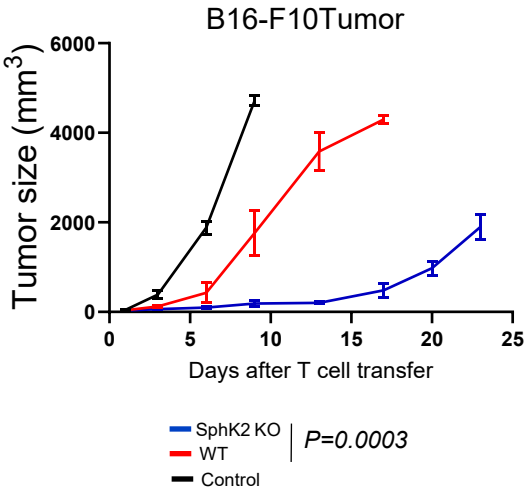
G
B16-F10Tumor
Tumor size (mm³)
Days after T cell transfer
SphK2 KO
WT
Control
P=0.0003

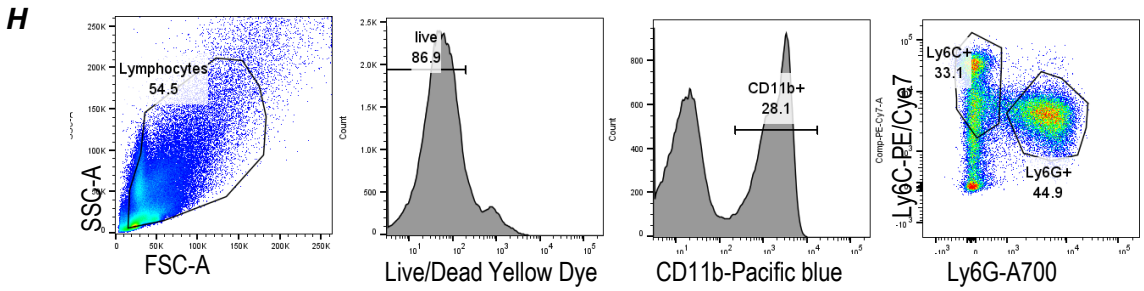
H
Lymphocytes
54.5
SSC-A
FSC-A
live
86.9
Count
Live/Dead Yellow Dye
CD11b+
28.1
CD11b-Pacific blue
Ly6C+
33.1
Ly6G+
44.9
Ly6C-PE/Cy7
Ly6G-A700

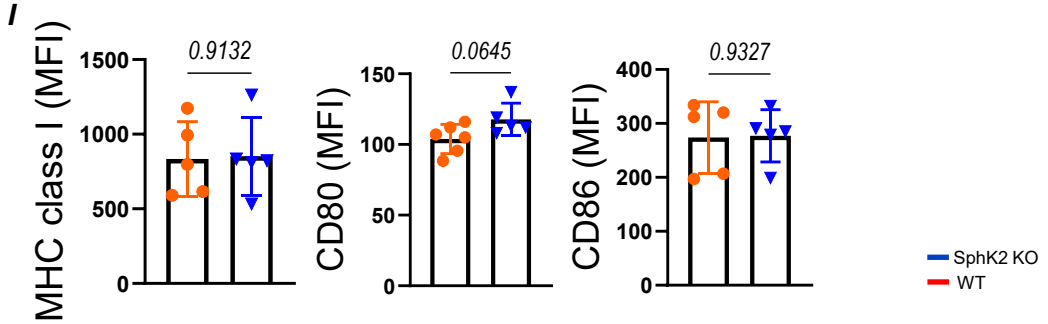
I
MHC class I (MFI)
0.9132
CD80 (MFI)
0.0645
CD86 (MFI)
0.9327
SphK2 KO
WT

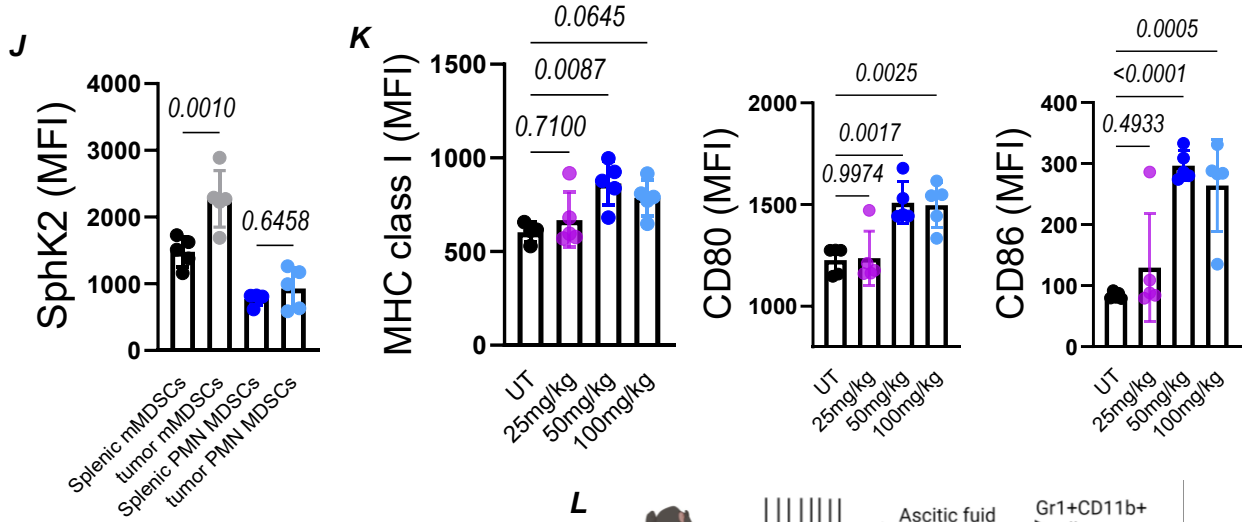
J
SphK2 (MFI)
0.0010
0.6458
Splenic mMDSCs
tumor mMDSCs
Splenic PMN MDSCs
tumor PMN MDSCs
K
MHC class I (MFI)
0.0645
0.0087
0.7100
CD80 (MFI)
0.0025
0.0017
0.9974
CD86 (MFI)
0.0005
<0.0001
0.4933
UT
25mg/kg
50mg/kg
100mg/kg

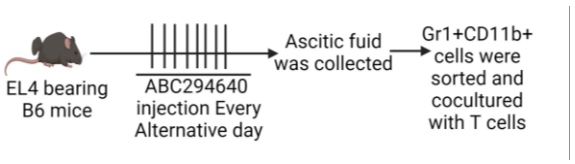
L
EL4 bearing
B6 mice
ABC294640
injection Every
Alternative day
Ascitic fuid
was collected
Gr1+CD11b+
cells were
sorted and
cocultured
with T cells

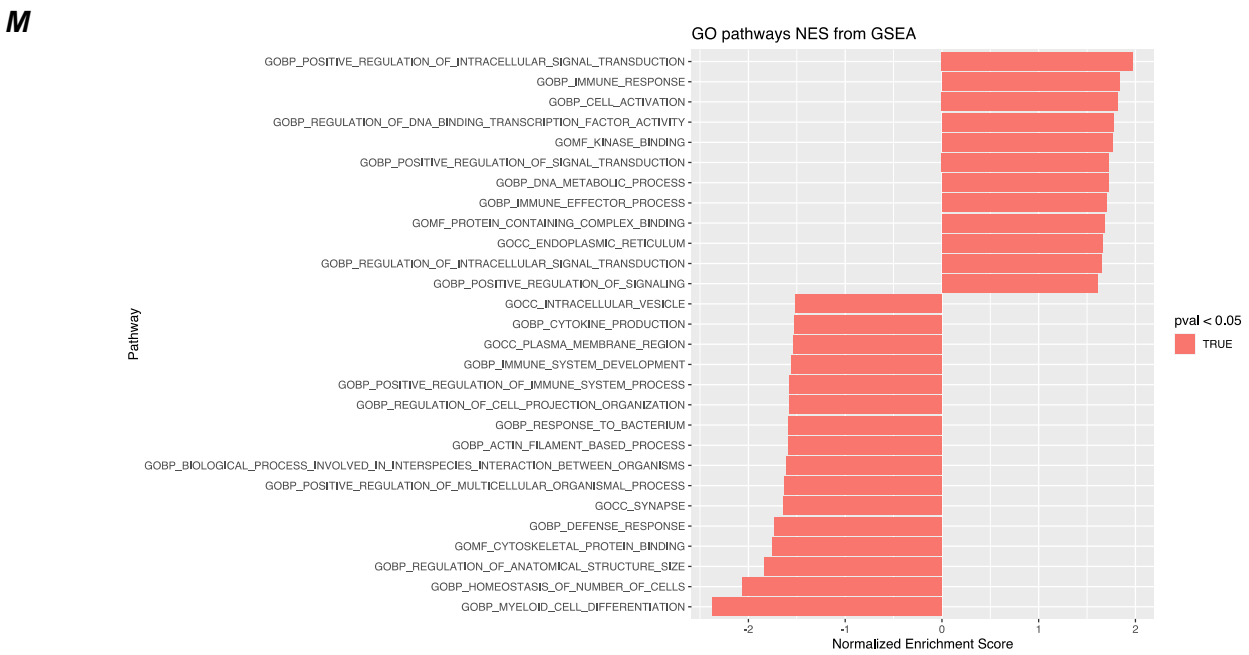
M
GO pathways NES from GSEA
GOBP_POSITIVE_REGULATION_OF_INTRACELLULAR_SIGNAL_TRANSDUCTION
GOBP_IMMUNE_RESPONSE
GOBP_CELL_ACTIVATION
GOBP_REGULATION_OF_DNA_BINDING_TRANSCRIPTION_FACTOR_ACTIVITY
GOMF_KINASE_BINDING
GOBP_POSITIVE_REGULATION_OF_SIGNAL_TRANSDUCTION
GOBP_DNA_METABOLIC_PROCESS
GOBP_IMMUNE_EFFECTOR_PROCESS
GOMF_PROTEIN_CONTAINING_COMPLEX_BINDING
GOCC_ENDOPLASMIC_RETICULUM
GOBP_REGULATION_OF_INTRACELLULAR_SIGNAL_TRANSDUCTION
GOBP_POSITIVE_REGULATION_OF_SIGNALING
GOCC_INTRACELLULAR_VESICLE
GOBP_CYTOKINE_PRODUCTION
GOCC_PLASMA_MEMBRANE_REGION
GOBP_IMMUNE_SYSTEM_DEVELOPMENT
GOBP_POSITIVE_REGULATION_OF_IMMUNE_SYSTEM_PROCESS
GOBP_REGULATION_OF_CELL_PROJECTION_ORGANIZATION
GOBP_RESPONSE_TO_BACTERIUM
GOBP_ACTIN_FILAMENT_BASED_PROCESS
GOBP_BIOLOGICAL_PROCESS_INVOLVED_IN_INTERSPECIES_INTERACTION_BETWEEN_ORGANISMS
GOBP_POSITIVE_REGULATION_OF_MULTICELLULAR_ORGANISMAL_PROCESS
GOCC_SYNAPSE
GOBP_DEFENSE_RESPONSE
GOMF_CYTOSKELETAL_PROTEIN_BINDING
GOBP_REGULATION_OF_ANATOMICAL_STRUCTURE_SIZE
GOBP_HOMEOSTASIS_OF_NUMBER_OF_CELLS
GOBP_MYELOID_CELL_DIFFERENTIATION
Pathway
Normalized Enrichment Score
pval < 0.05
TRUE

N

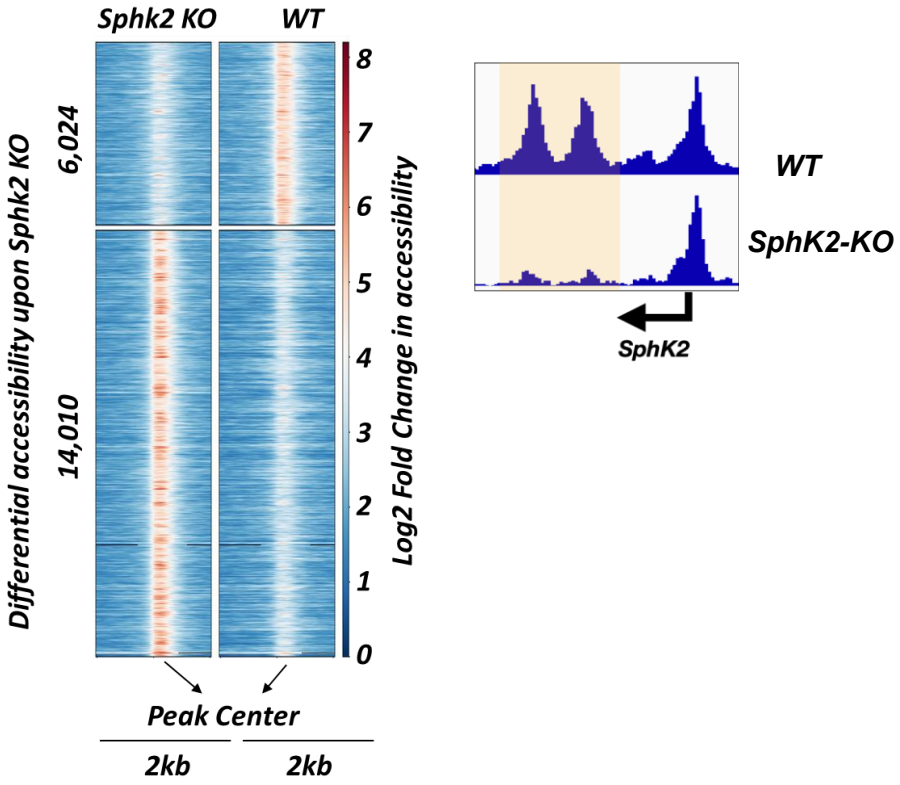
Sphk2 KO
WT
Differential accessibility upon Sphk2 KO
6,024
14,010
8
7
6
5
4
3
2
1
0
Log2 Fold Change in accessibility
Peak Center
2kb
2kb
WT
SphK2-KO
SphK2

O

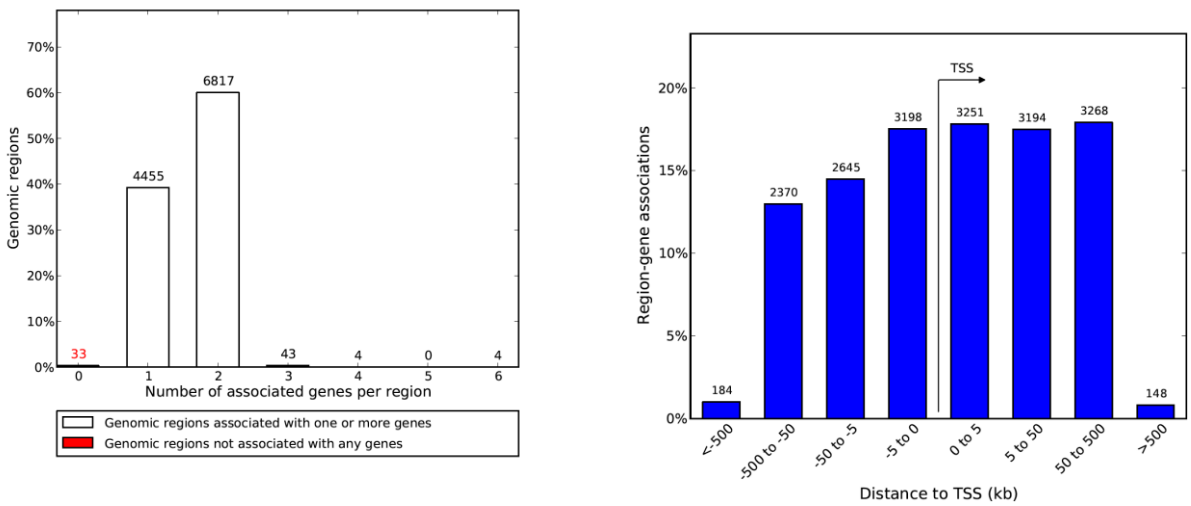
Genomic regions
70%
60%
50%
40%
30%
20%
10%
0%
33
4455
6817
43
4
0
4
0
1
2
3
4
5
6
Number of associated genes per region
Genomic regions associated with one or more genes
Genomic regions not associated with any genes
Region-gene associations
20%
15%
10%
5%
0%
184
2370
2645
3198
3251
3194
3268
148
TSS
<-500
-500 to -50
-50 to -5
-5 to 0
0 to 5
5 to 50
50 to 500
>500
Distance to TSS (kb)

P

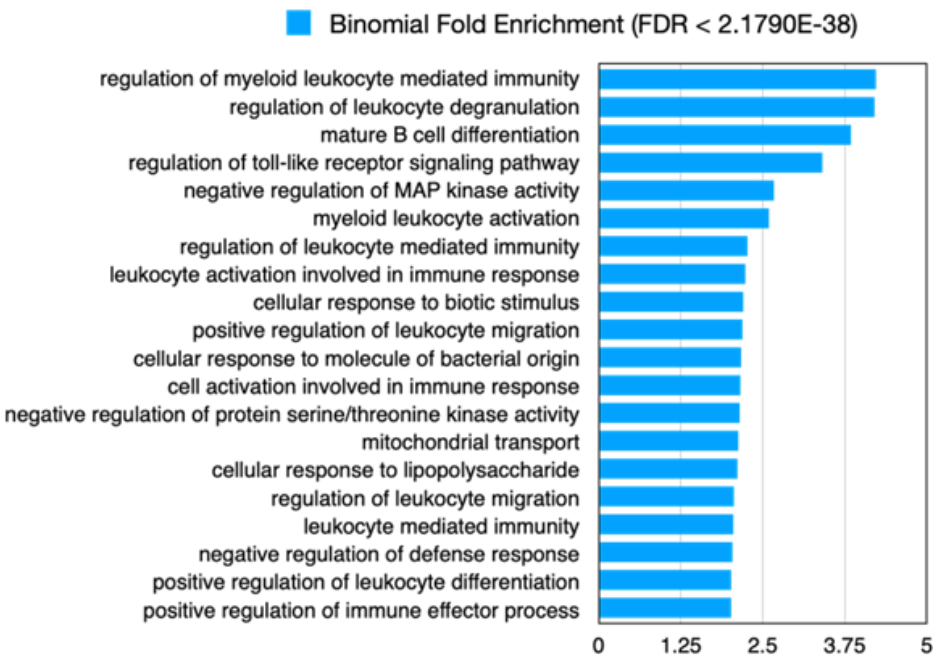
Binomial Fold Enrichment (FDR < 2.1790E-38)
regulation of myeloid leukocyte mediated immunity
regulation of leukocyte degranulation
mature B cell differentiation
regulation of toll-like receptor signaling pathway
negative regulation of MAP kinase activity
myeloid leukocyte activation
regulation of leukocyte mediated immunity
leukocyte activation involved in immune response
cellular response to biotic stimulus
positive regulation of leukocyte migration
cellular response to molecule of bacterial origin
cell activation involved in immune response
negative regulation of protein serine/threonine kinase activity
mitochondrial transport
cellular response to lipopolysaccharide
regulation of leukocyte migration
leukocyte mediated immunity
negative regulation of defense response
positive regulation of leukocyte differentiation
positive regulation of immune effector process
0
1.25
2.5
3.75
5

Supplementary Figure 1: A) Gating strategy used to identify $Gr1^+CD11b^+$ mouse from the tumor and spleens. ***B)*** EL-4 tumor was established in C57BL/6 mice for two weeks. TILs and splenocytes were isolated from healthy or EL-4 tumor-bearing mice, and flow cytometry-based determination of intracellular SphK1 expression in $Gr1^+CD11b^+$ MDSCs was performed. The TILs were also used to determine the expression of SphK2 in $Gr1^+CD11b^+$ MDSCs (***C)***. n= 5 mice/group.

D*)* T-SNE plot of different immune cell types from the scRNA-seq data of GEM models of aggressive breast cancer, representing TNBC.

E) EL-4 tumor was established in WT, *SphK1*-KO, and *SphK2*-KO mice for two weeks. FACS-sorted MDSCs ($Gr1^+CD11b^+$) from the ascitic tumor site were co-cultured with CTV-labeled T cells at 1:2 MDSC: T cell ratio for 72h in the presence of anti-CD3/anti-CD28 antibody (each 2 ug/ml). Cell proliferation was evaluated by flow cytometry. ***F)*** SphK2 expression (MFI) in M-MDSCs from spleen and tumors of B16-F10 tumor–bearing mice at different tumor sizes. n = 5 mice/group.

G) B16-F10 murine melanoma was established either in WT or *SphK2*-KO mice. After nine days of tumor establishment, Pmel T cells were injected into the tumor-bearing mice, and tumor growth was monitored. Tumor growth curves represent mean tumor volume ± SEM. n = 6 mice/group.

H) EL-4 ascites-derived MDSCs from WT and *SphK2*-KO mice. Gating strategy used to identify $Ly6C^{high}$ $Ly6G^{low}$ M-MDSCs and ($Ly6C^{low}Ly6G^{high}$) PMN-MDSCs from the tumor and spleens ***(I)***. PMN ($Ly6C^{low}Ly6G^{high}$) MDSCs were phenotypically characterized by using flow cytometry for the indicated surface molecules. ***J)*** SphK2 expression (MFI) was measured in monocytic (M-MDSCs) and polymorphonuclear (PMN-MDSCs) MDSCs from the spleen and tumors of EL-4 tumor–bearing mice. ***K)*** EL-4 tumor–bearing mice were treated with the ABC294640 (*SphK2i*) at the indicated doses for 2 weeks. Expression of the indicated markers on MDSCs was analyzed by flow cytometry. n = 5 mice/group.

L) EL-4 tumor was established for 5 days in C57BL/6 mice. The tumor-bearing mice were treated with ABC294640 (50 mg/kg) for two weeks. The schematic for the experiment is shown (*Created in BioRender. MEHROTRA, S. (2026) https: l/BioRender.coml i20a424*).

M) EL-4 tumor was established in C57BL/6 mice for two weeks. $Gr1^+CD11b^+$ MDSCs were isolated, and RNA-seq analysis was performed. n = 2 biologically independent samples per group, pooled from 4 mice per group. ***N)*** $Gr1^+CD11b^+$ MDSCs were also used to perform ATAC-seq analysis. ATAC-seq heatmaps and aggregate plots showing chromatin accessibility around peak centers (±2 kb); the *SphK2* locus is indicated by the arrow. n = 2 biologically independent samples per group, pooled from 4 mice per group. ***O)*** Genomic region–gene association distribution (left) and distance of ATAC-seq peaks to transcription start sites (TSS: right panel). ***P)*** Gene Ontology enrichment of genes associated with accessible chromatin regions.

Data is presented as mean ± SD. Statistical significance was determined using an unpaired two-tailed Student's t test for comparisons between two groups and one-way ANOVA with Šídák's multiple comparisons test for multiple group comparisons.

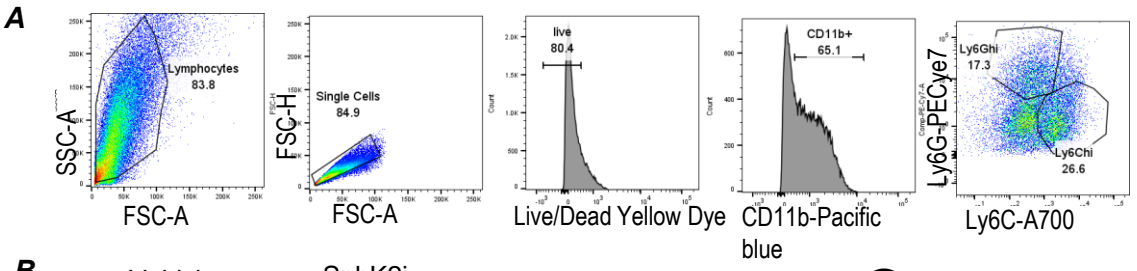
A
Lymphocytes
83.8
SSC-A
FSC-A
Single Cells
84.9
FSC-H
FSC-A
live
80.4
Live/Dead Yellow Dye
CD11b+
65.1
CD11b-Pacific blue
Ly6Ghi
17.3
Ly6Chi
26.6
Ly6G-PECye7
Ly6C-A700

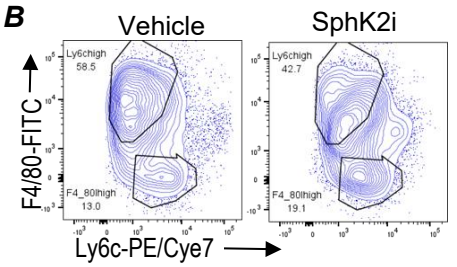
B
Vehicle
SphK2i
Ly6chigh
58.5
F4_80lhigh
13.0
Ly6chigh
42.7
F4_80lhigh
19.1
F4/80-FITC
Ly6c-PE/Cye7

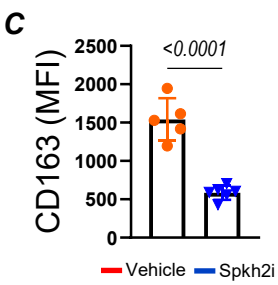
C
<0.0001
CD163 (MFI)
2500
2000
1500
1000
500
0
Vehicle
Spkh2i

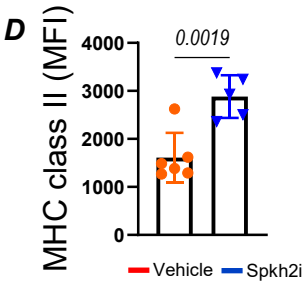
D
0.0019
MHC class II (MFI)
4000
3000
2000
1000
0
Vehicle
Spkh2i

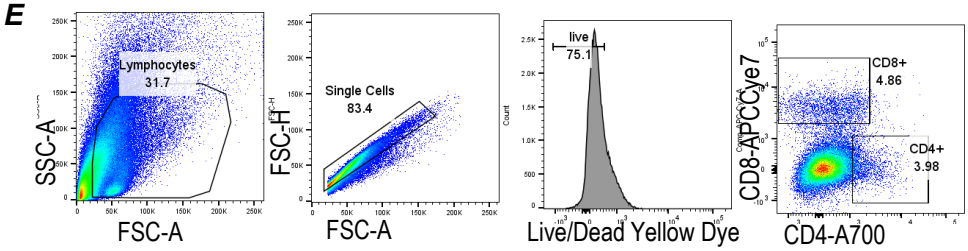
E
Lymphocytes
31.7
SSC-A
FSC-A
Single Cells
83.4
FSC-H
FSC-A
live
75.1
Live/Dead Yellow Dye
CD8+
4.86
CD4+
3.98
CD8-APCCye7
CD4-A700

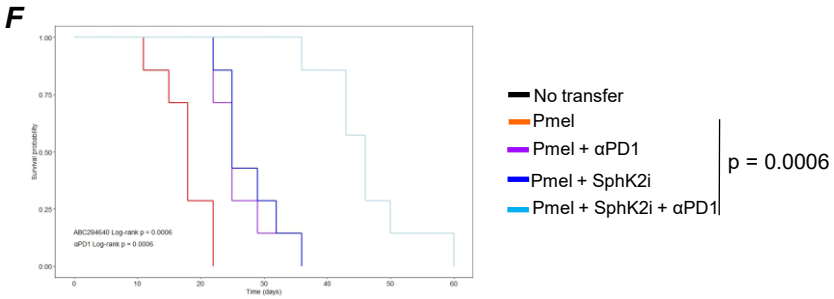
F
No transfer
Pmel
Pmel + αPD1
Pmel + SphK2i
Pmel + SphK2i + αPD1
p = 0.0006

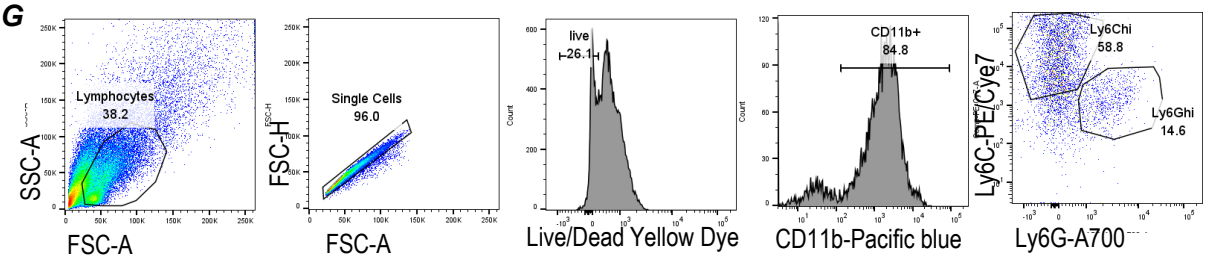
G
Lymphocytes
38.2
SSC-A
FSC-A
Single Cells
96.0
FSC-H
FSC-A
live
26.1
Live/Dead Yellow Dye
CD11b+
84.8
CD11b-Pacific blue
Ly6Chi
58.8
Ly6Ghi
14.6
Ly6G-PECye7
Ly6G-A700

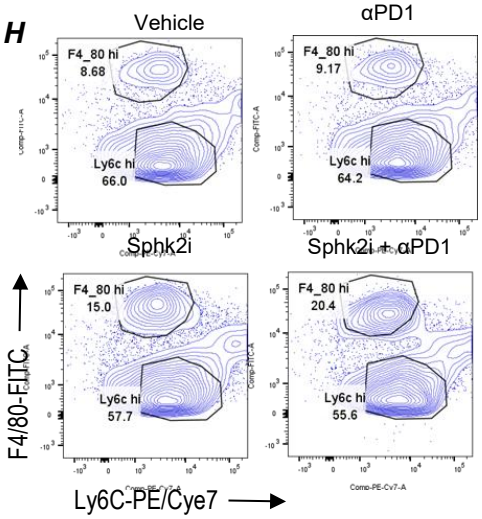
H
Vehicle
αPD1
F4_80 hi
8.68
Ly6c hi
66.0
F4_80 hi
9.17
Ly6c hi
64.2
Sphk2i
Sphk2i + αPD1
F4_80 hi
15.0
Ly6c hi
57.7
F4_80 hi
20.4
Ly6c hi
55.6
F4/80-FITC
Ly6C-PE/Cye7

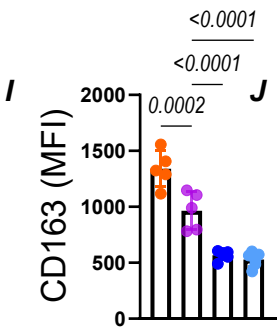
I
<0.0001
<0.0001
0.0002
CD163 (MFI)
2000
1500
1000
500
0

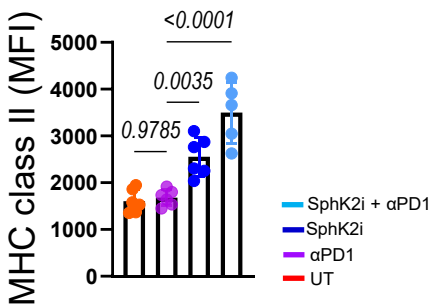
J
<0.0001
0.0035
0.9785
MHC class II (MFI)
5000
4000
3000
2000
1000
0
SphK2i + αPD1
SphK2i
αPD1
UT

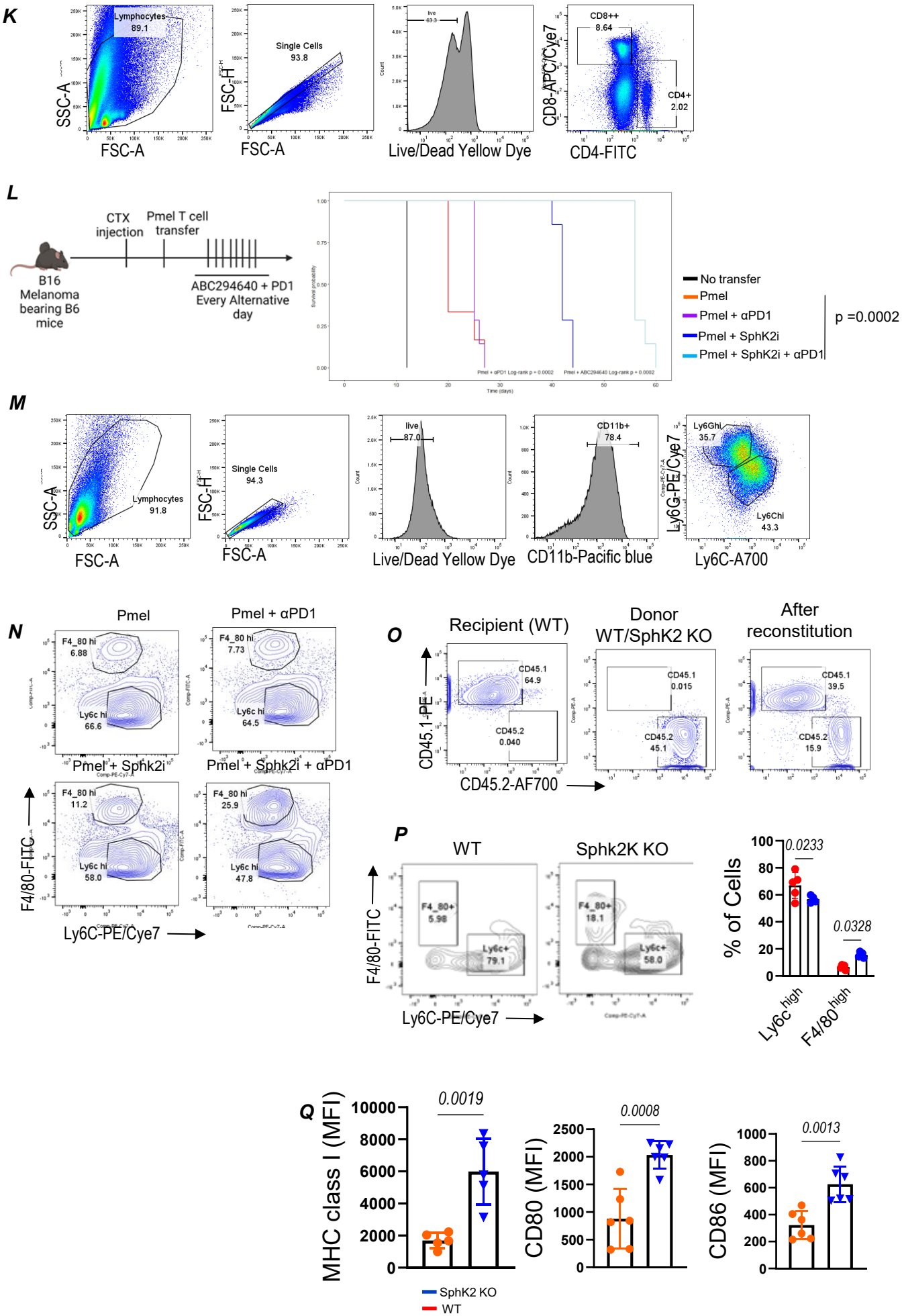
K
Lymphocytes
89.1
SSC-A
FSC-A
Single Cells
93.8
FSC-H
FSC-A
live
63.3
Count
Live/Dead Yellow Dye
CD8++
8.64
CD4+
2.02
CD8-APC/Cye7
CD4-FITC
L
CTX injection
Pmel T cell transfer
B16 Melanoma bearing B6 mice
ABC294640 + PD1 Every Alternative day
Survival probability
Time (days)
Pmel + αPD1 Log-rank p = 0.0002
Pmel + ABC294640 Log-rank p = 0.0002
No transfer
Pmel
Pmel + αPD1
Pmel + SphK2i
Pmel + SphK2i + αPD1
p =0.0002
M
Lymphocytes
91.8
SSC-A
FSC-A
Single Cells
94.3
FSC-H
FSC-A
live
87.0
Count
Live/Dead Yellow Dye
CD11b+
78.4
CD11b-Pacific blue
Ly6Ghi
35.7
Ly6Chi
43.3
Ly6G-PE/Cye7
Ly6C-A700
N
Pmel
Pmel + αPD1
F4_80 hi
6.88
Ly6c hi
66.6
F4_80 hi
7.73
Ly6c hi
64.5
Pmel + Sphk2i
Pmel + Sphk2i + αPD1
F4_80 hi
11.2
Ly6c hi
58.0
F4_80 hi
25.9
Ly6c hi
47.8
F4/80-FITC
Ly6C-PE/Cye7
O
Recipient (WT)
Donor WT/SphK2 KO
After reconstitution
CD45.1
64.9
CD45.2
0.040
CD45.1
0.015
CD45.2
45.1
CD45.1
39.5
CD45.2
15.9
CD45.1-PE
CD45.2-AF700
P
WT
Sphk2K KO
F4_80+
5.98
Ly6c+
79.1
F4_80+
18.1
Ly6c+
58.0
F4/80-FITC
Ly6C-PE/Cye7
% of Cells
0.0233
0.0328
Ly6c high
F4/80 high
Q
MHC class I (MFI)
0.0019
CD80 (MFI)
0.0008
CD86 (MFI)
0.0013
SphK2 KO
WT

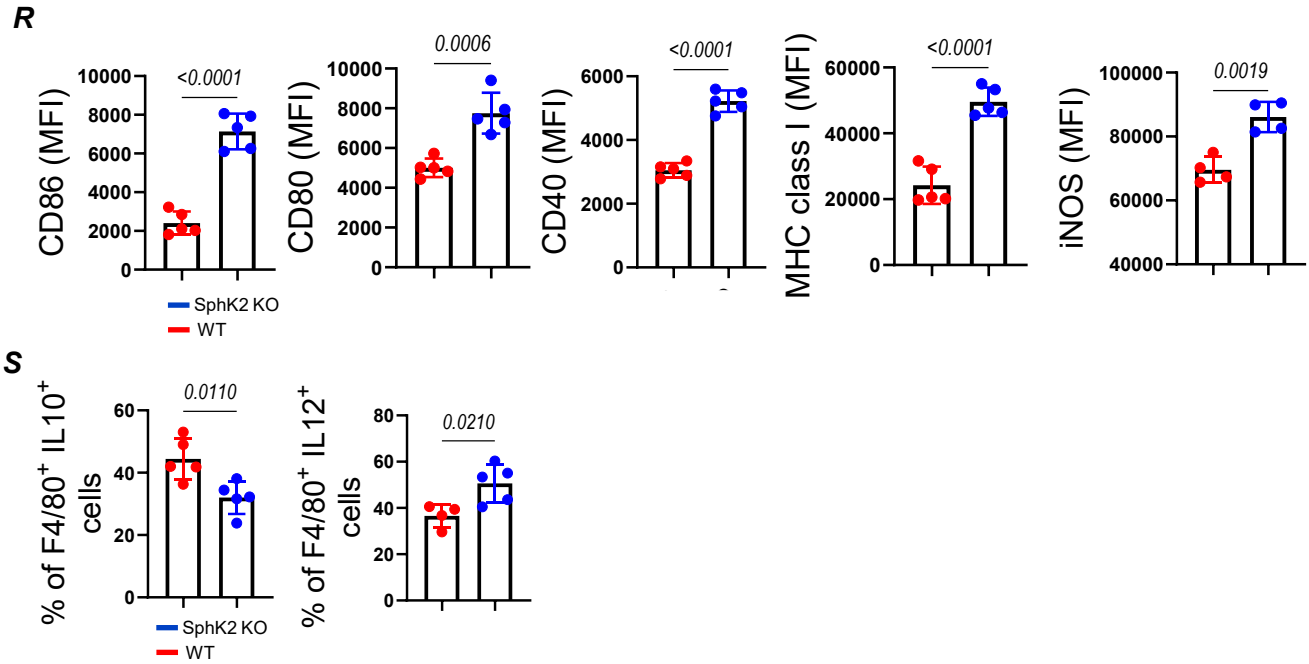

Supplementary Figure 2: A) Gating strategy used to identify Ly6C^{high} Ly6G^{low} M-MDSCs from the 4T1 tumor. ***B)*** 4T1 tumor was established in BALB/c mice. Nine days after tumor injection, mice were injected with vehicle or ABC294640 (*Sphk2i*: 50 mg/kg). Cells obtained from the tumor site were analyzed for the differentiation of Ly6C^{high} M-MDSCs into F4/80^{high} macrophages. CD163 ***(C),*** and MHC Class II ***(D)*** expression was checked in F4/80^{high} macrophages. ***E)*** Gating strategy used to identify CD4^{+} and CD8^{+} T cells from the 4T1 tumor. (n = 5 mice /group).

F) MB-49 bladder tumor cells were injected into C57BL/6 mice, and tumor-bearing mice were either treated with vehicle or *Sphk2i* (50 mg/kg). Survival curves were analyzed using the Kaplan–Meier method, and statistical significance was determined using the log-rank test (n = 7 mice /group). Gating strategy used to identify Ly6C^{high} Ly6G^{low} M-MDSCs from the MB-49 tumor ***(G)***. ***H)*** Cells obtained from the tumor site were analyzed for the differentiation of Ly6C^{high} M-MDSCs into F4/80^{high} macrophages. CD163 ***(I)*** and MHC Class II ***(J)*** expression was checked in F4/80^{high} macrophages. ***K)*** Gating strategy used to identify CD4^{+} and CD8^{+} T cells from the MB-49 tumor. (n = 5 mice /group).

L) Subcutaneously established B16-F10 melanoma was treated with gp100 reactive Pmel T cells along with *Sphk2i* and anti-PD1 antibody (200 μg/mouse every alternate day), and tumor growth was monitored. *Left panel* shows the schematic for the adoptive transfer experiment (*Created in BioRender. MEHROTRA, S. (2026) https: l/BioRender.coml i20a424*). The *right panel* shows Kaplan–Meier survival curves of tumor-bearing mice treated with the indicated regimens (n = 7 mice/group). Gating strategy used to identify Ly6C^{high} Ly6G^{low} M-MDSCs from the B16-F10 tumor ***(M)***. ***N)*** Cells obtained from the tumor site (M) were analyzed for the differentiation of Ly6C^{high} M-MDSCs into F4/80^{high} macrophages. (n = 5 mice /group).

O) WT or SphK2 KO (CD45.2^{+}) MDSCs generated *in vitro* for 4 days were adoptively transferred into CD45.1^{+} B16 tumor–bearing mice (day 12 after tumor establishment). Five days after transfer, tumors were harvested and analyzed by flow cytometry for donor cell engraftment (CD45.2), Ly6C^{high} M-MDSCs into F4/80^{high} macrophages. ***(P)***, and expression of the indicated markers (CD80, CD86, MHC class I) on M-MDSCs ***(Q)***. (n = 5 mice /group).

R) Bone marrow cells from WT and *SphK2*-KO mice were isolated and cultured in the presence of M-CSF (20ng/ml) and 30% B16-F10 tumor explant supernatant for seven days to generate macrophages. F4/80^{+} macrophages obtained after seven days of incubation were evaluated for the indicated immunostimulatory markers by flow cytometry. ***S)*** Cells from (R) were activated with LPS overnight, and intracellular secretion of IL-10 and IL-12 was determined. (n = 5 mice /group).

Data is presented as mean ± SD. Statistical significance was determined using an unpaired two-tailed Student's t test for comparisons between two groups and one-way ANOVA with Šídák's multiple comparisons test for multiple group comparisons.

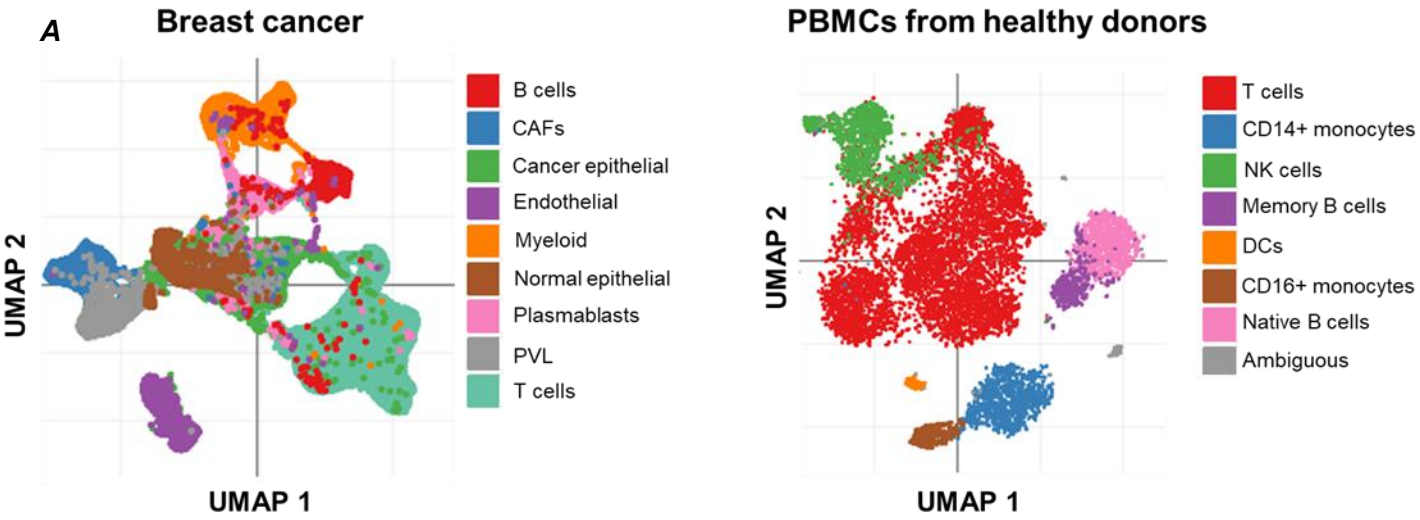

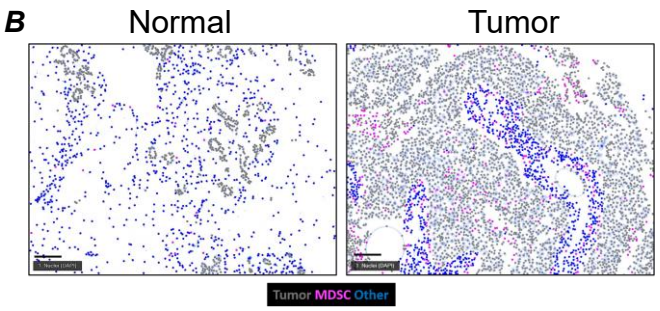

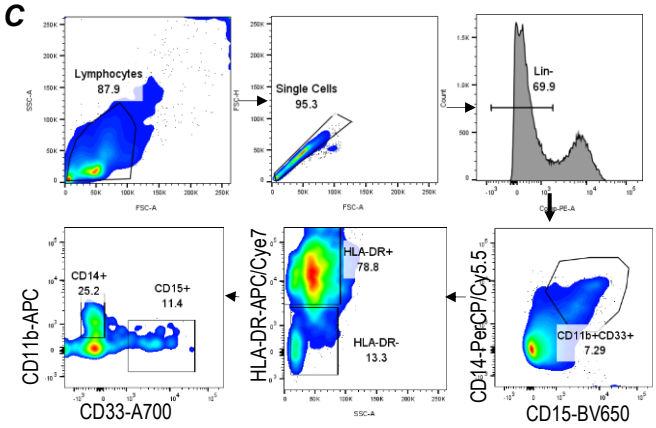

D Analysis of the immune profiling in SphK2i (Opaganib/ABC294640) trial

Table 1: Average (SD) percentage of cells positive for a given marker at baseline and EOT, and summary of change from baseline to EOT (n = 30).

Cell type	Baseline	EOT	Δ = EOT - Baseline		
	Mean (SD)	Mean (SD)	Mean (SD)	95% CI	p-value*
Mo-MDSC	21.6 (19.4)	11.7 (11.8)	-9.8 (22.0)	(-18.0, -1.6)	0.02
IFNg+ T Cells	10.6 (8.6)	17.0 (14.7)	6.4 (14.0)	(1.2, 11.6)	0.02
Gzmb+ T Cells	47.4 (24.4)	60.8 (22.6)	13.4 (25.2)	(4.0, 22.8)	0.0007

Abbreviations: CI = confidence interval; EOT = end of treatment; SD = standard deviation
***p-value based on paired t-test**

The table summarizes the average (standard deviation [SD]) of the percentage of cells of a given type measured at baseline (pre-treatment) and end of treatment (EOT). Change scores (Δ = EOT – baseline) were calculated to evaluate the absolute increase or decrease in the percentage of cells of each type. Average change score (SD) and corresponding 95% confidence interval (CI) are reported for each cell type. A positive (negative) average change score reflects an increase (decrease) in the percentage of cells from baseline to EOT. We used histograms and quantile-quantile plots to evaluate the approximate normality of change scores (not shown), and a paired t-test to test the null hypothesis that the average change in the percentage of cells is 0 versus the alternative that the average change differs significantly from 0. All average change scores differ significantly from 0. The accompanying figure shows boxplots of change scores for each cell type.

- The percentage of Mo-MDSC significantly decreased in response to opaganib treatment (average change = -9.8, 95% CI = -18.0 to -1.6; p = 0.02).
- The percentage of IFNγ+ T cells significantly increased in response to opaganib treatment (average change = 6.4, 95% CI = 1.2 to 11.6; p = 0.02).
- The percentage of Gzmb+ T cells significantly increased in response to opaganib treatment (average change = 13.4, 95% CI = 4.0 to 22.8; p = 0.0007).

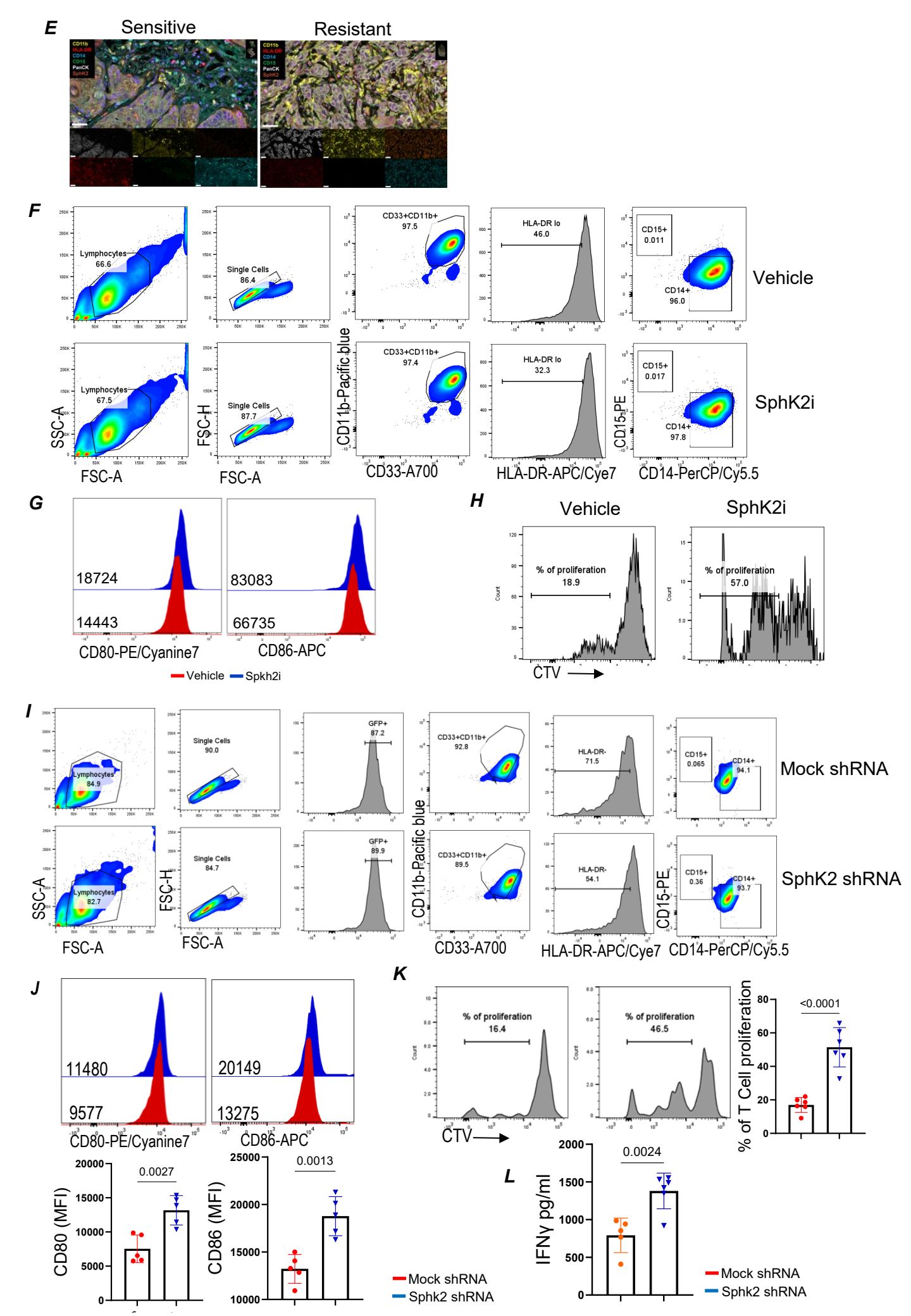
E
Sensitive
Resistant
CD11b
HLA-DR
CD14
CD15
PanCK
SphK2
F
Lymphocytes
66.6
Single Cells
86.4
CD33+CD11b+
97.5
HLA-DR lo
46.0
CD15+
0.011
CD14+
96.0
Vehicle
Lymphocytes
67.5
Single Cells
87.7
CD33+CD11b+
97.4
HLA-DR lo
32.3
CD15+
0.017
CD14+
97.8
SphK2i
SSC-A
FSC-A
FSC-H
FSC-A
CD11b-Pacific blue
CD33-A700
HLA-DR-APC/Cye7
CD15-PE
CD14-PerCP/Cy5.5
G
18724
14443
83083
66735
CD80-PE/Cyanine7
CD86-APC
Vehicle
Spkh2i
H
Vehicle
SphK2i
% of proliferation
18.9
% of proliferation
57.0
Count
CTV
I
Lymphocytes
84.9
Single Cells
90.0
GFP+
87.2
CD33+CD11b+
92.8
HLA-DR-
71.5
CD15+
0.065
CD14+
94.1
Mock shRNA
Lymphocytes
82.7
Single Cells
84.7
GFP+
89.9
CD33+CD11b+
89.5
HLA-DR-
54.1
CD15+
0.36
CD14+
93.7
SphK2 shRNA
SSC-A
FSC-A
FSC-H
FSC-A
CD11b-Pacific blue
CD33-A700
HLA-DR-APC/Cye7
CD15-PE
CD14-PerCP/Cy5.5
J
11480
9577
20149
13275
CD80-PE/Cyanine7
CD86-APC
0.0027
0.0013
CD80 (MFI)
CD86 (MFI)
Mock shRNA
Sphk2 shRNA
K
% of proliferation
16.4
% of proliferation
46.5
CTV
<0.0001
% of T Cell proliferation
L
0.0024
IFNγ pg/ml
Mock shRNA
Sphk2 shRNA

Supplementary Figure 3: A) UMAP plots of different cell clusters from the scRNA-seq data of breast cancer patients and PBMCs from healthy donors. ***B)*** Representative cellular phenotype images in normal breast tissues and triple-negative breast tumors showing the spatial location of cells resembling MDSCs ($pCK^{neg}HLA\text{-}DR^{neg}CD11b+CD14+CD15^{neg}$; pink dots), pCK^{pos} tumor cells (grey dots), and undefined stromal cells pCK^{neg} (blue dots). Scale bar, 100µm. ***C)*** A representative gating strategy is used to identify M-MDSC and PMN-MDSC from the peripheral blood of prostate cancer patients and healthy controls. ***D)*** Table summarizes the average (standard deviation [SD]) of the percentage of cells of a given type measured at baseline (pre-treatment) and end of treatment (EOT). ***E)*** Representative multispectral immunofluorescence images of oral cavity squamous cell carcinoma (OCSCC) tumor sections from anti–PD-1–sensitive and –resistant patients, showing SphK2 expression in $CD11b^{+}HLA\text{-}DR^{low}CD14^{+}CD15^{-}$ monocytic MDSCs. Scale bar, wide field 40µm; single channel 40µm. ***F)*** Gating strategy used to identify monocytic human MDSCs following treatment with or without *Sphk2i*. ***(G)*** Overlay histograms showing surface expression of the indicated markers on MDSCs with or without *Sphk2i* treatment. ***(H)*** *Sphk2i*-treated or untreated MDSCs were co-cultured with CTV-labeled autologous T cells at a 1:4 ratio. T cell proliferation was assessed by flow cytometry. ***(I)*** Human MDSCs transduced with control (MOCK) or SphK2 shRNA were identified based on GFP expression. Gating strategy is shown to delineate monocytic MDSCs following transduction. ***(J)*** Overlay histograms showing surface expression of the indicated markers on MDSCs treated with either MOCK or SphK2 shRNA. Graphs represent cumulative data from independent experiments. ***(K)*** MOCK or SphK2 shRNA-transduced MDSCs were co-cultured with CTV-labeled autologous T cells at a 1:4 ratio, and T cell proliferation was assessed by flow cytometry. Graphs represent cumulative data from multiple experiments. ***(L)*** IFN-γ levels in the co-culture supernatants were measured by ELISA.

Data is presented as mean ± SD of n = 5 independent experiments unless otherwise specified. Statistical significance was determined using an unpaired two-tailed Student's *t*-test.

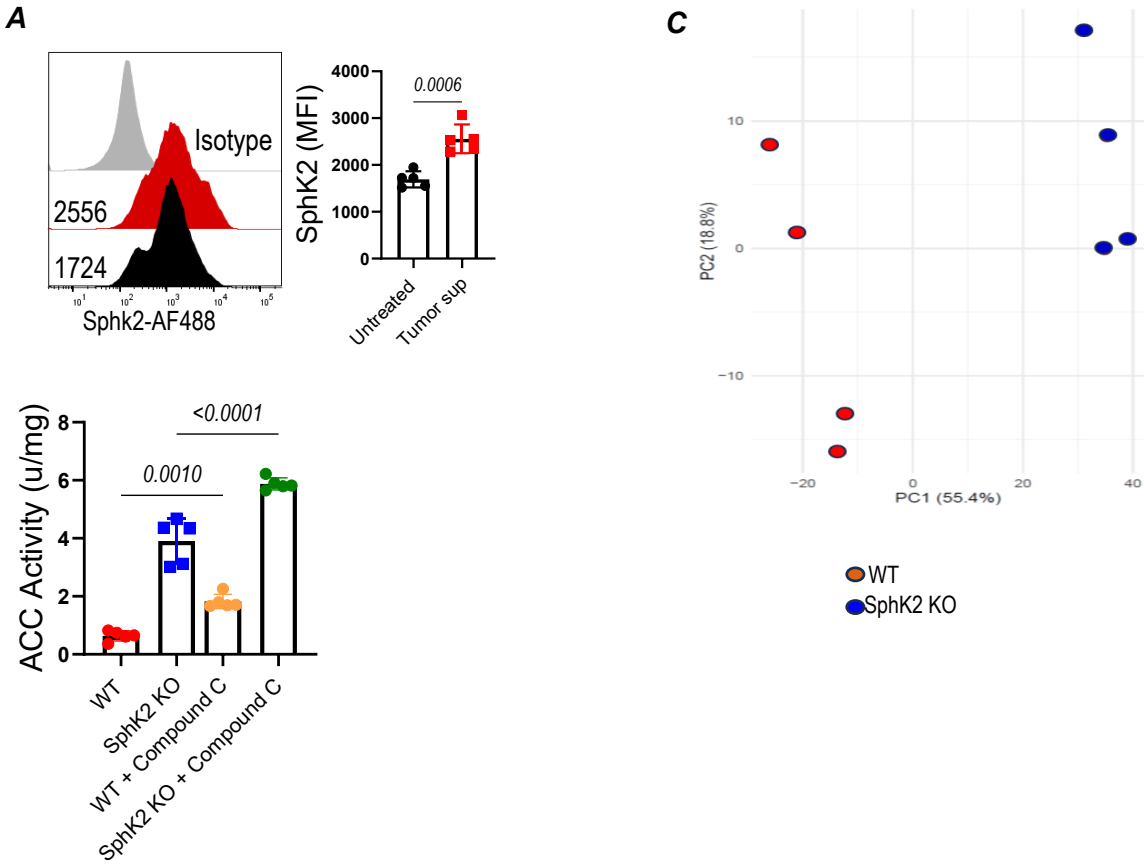

Supplementary Figure 4: A) Bone marrow cells from WT mice were isolated and cultured in the presence of GM-CSF (20ng/ml) and 30% B16-F10 tumor explant supernatant for four days. Sphk2 expression was checked by flow cytometry in $Gr1^+$ $CD11b^+$ MDSCs. Statistical significance was determined using an unpaired two-tailed Student's *t*-test. Data is presented as mean ± SD of n = 5 independent experiments. ***B)*** Bone marrow cells from WT and *SphK2*-KO mice were isolated and cultured with GM-CSF (20 ng/mL) and 30% B16-F10 tumor explant supernatant (TES) for four days with and without treatment with the compound C (2 µM) for the last 12 hours. ACC activity was measured as per the manufacturer's protocol. Statistical significance was determined using one-way ANOVA with Šídák's multiple comparisons test for multiple group comparisons. Data is presented as mean ± SD of n = 5 independent experiments.

C) WT vs. *SphK2*-KO MDSCs were generated as described in (*A*). Untargeted lipidomic profiling was performed using LC-MS on four biological replicates per group and principal component analysis was performed (n=4 mice/group).

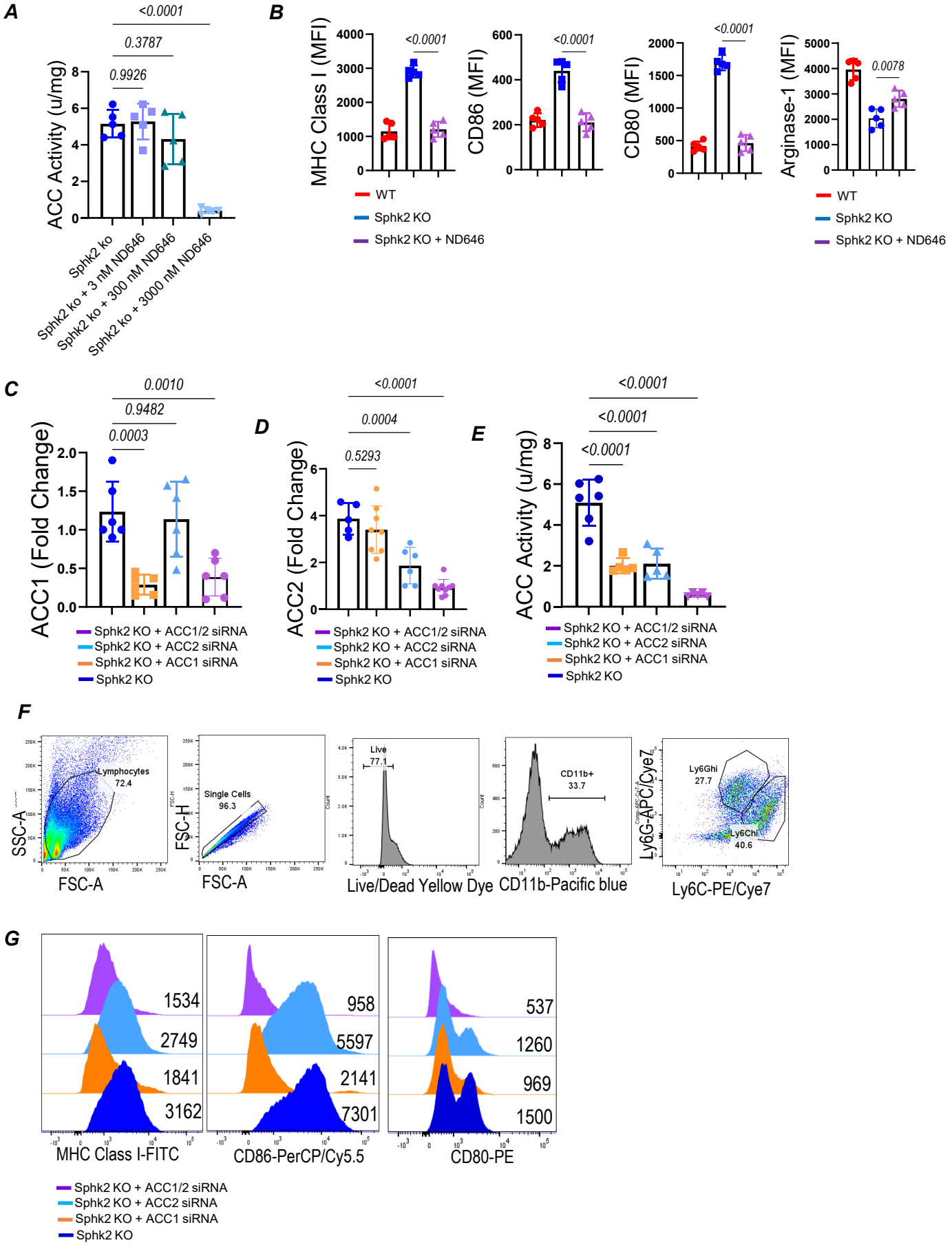
A
<0.0001
0.3787
0.9926
ACC Activity (u/mg)
Sphk2 ko
Sphk2 ko + 3 nM ND646
Sphk2 ko + 300 nM ND646
Sphk2 ko + 3000 nM ND646
B
MHC Class I (MFI)
CD86 (MFI)
CD80 (MFI)
Arginase-1 (MFI)
<0.0001
0.0078
WT
Sphk2 KO
Sphk2 KO + ND646
C
0.0010
0.9482
0.0003
ACC1 (Fold Change)
D
<0.0001
0.0004
0.5293
ACC2 (Fold Change)
E
<0.0001
ACC Activity (u/mg)
Sphk2 KO + ACC1/2 siRNA
Sphk2 KO + ACC2 siRNA
Sphk2 KO + ACC1 siRNA
Sphk2 KO
F
Lymphocytes
72.4
SSC-A
FSC-A
Single Cells
96.3
FSC-H
Live
77.1
Live/Dead Yellow Dye
CD11b+
33.7
CD11b-Pacific blue
Ly6Ghi
27.7
Ly6Chi
40.6
Ly6G-APC/Cye7
Ly6C-PE/Cye7
G
1534
2749
1841
3162
MHC Class I-FITC
958
5597
2141
7301
CD86-PerCP/Cy5.5
537
1260
969
1500
CD80-PE
Sphk2 KO + ACC1/2 siRNA
Sphk2 KO + ACC2 siRNA
Sphk2 KO + ACC1 siRNA
Sphk2 KO

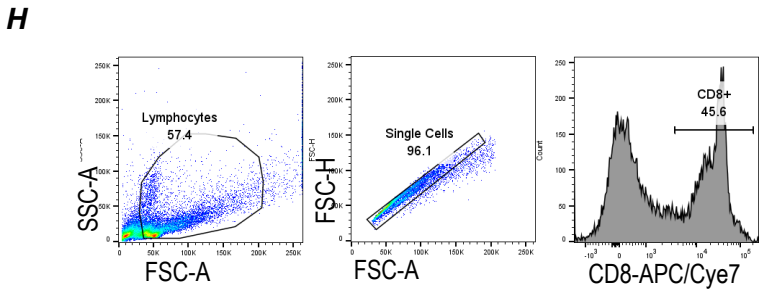
H
Lymphocytes
57.4
SSC-A
FSC-A
Single Cells
96.1
FSC-H
FSC-A
CD8+
45.6
CD8-APC/Cye7

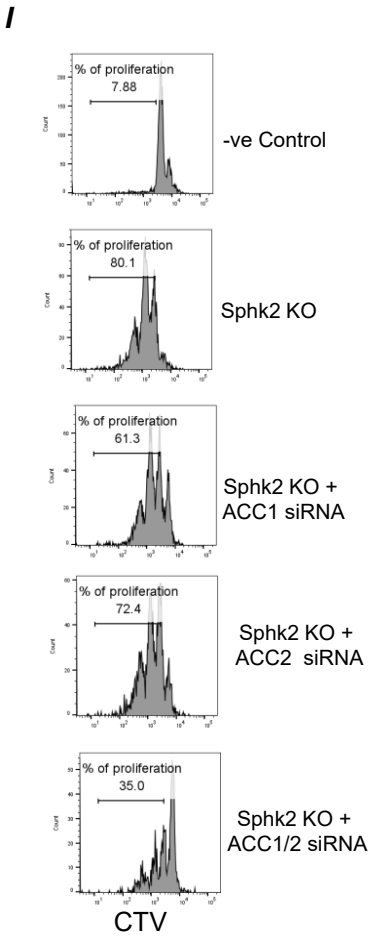
I
% of proliferation
7.88
-ve Control
% of proliferation
80.1
Sphk2 KO
% of proliferation
61.3
Sphk2 KO +
ACC1 siRNA
% of proliferation
72.4
Sphk2 KO +
ACC2 siRNA
% of proliferation
35.0
Sphk2 KO +
ACC1/2 siRNA
CTV

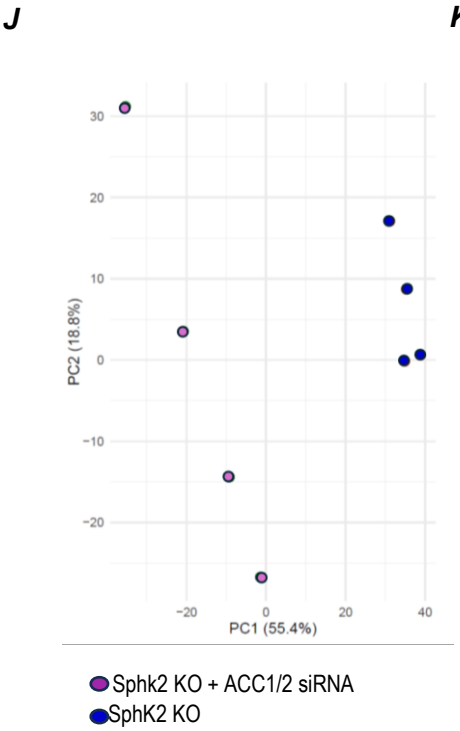
J
PC2 (18.8%)
PC1 (55.4%)
Sphk2 KO + ACC1/2 siRNA
SphK2 KO

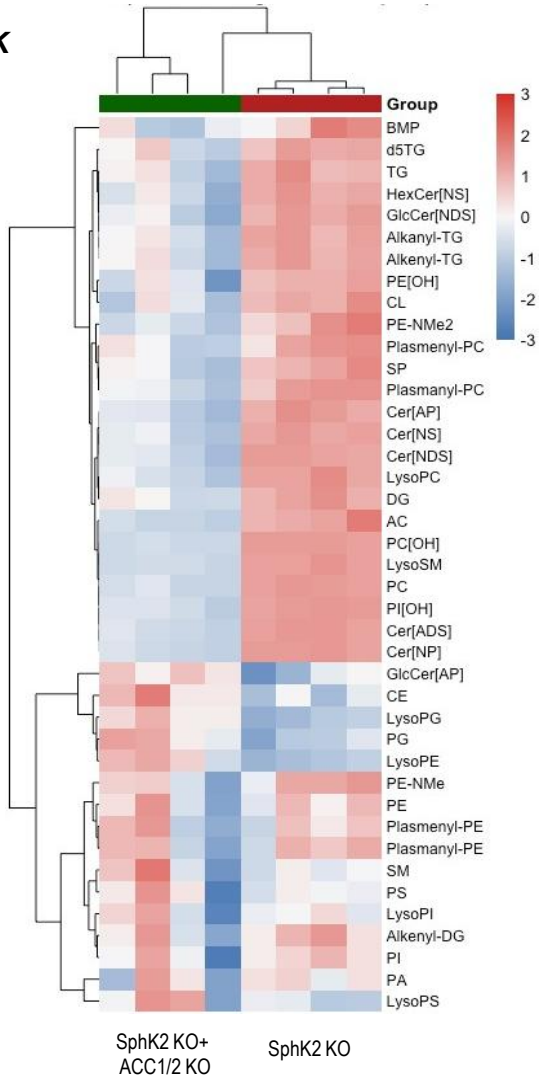
K
Group
BMP
d5TG
TG
HexCer[NS]
GlcCer[NDS]
Alkanyl-TG
Alkenyl-TG
PE[OH]
CL
PE-NMe2
Plasmenyl-PC
SP
Plasmanyl-PC
Cer[AP]
Cer[NS]
Cer[NDS]
LysoPC
DG
AC
PC[OH]
LysoSM
PC
PI[OH]
Cer[ADS]
Cer[NP]
GlcCer[AP]
CE
LysoPG
PG
LysoPE
PE-NMe
PE
Plasmenyl-PE
Plasmanyl-PE
SM
PS
LysoPI
Alkenyl-DG
PI
PA
LysoPS
SphK2 KO+
ACC1/2 KO
SphK2 KO

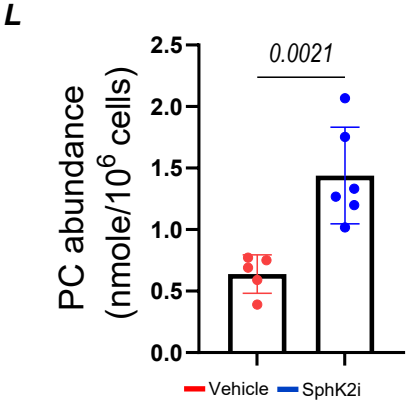
L
0.0021
PC abundance
(nmole/10^6 cells)
Vehicle
SphK2i

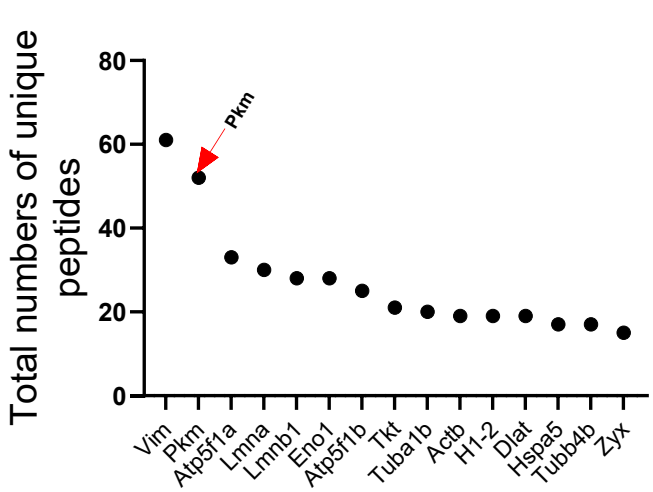
M
Total numbers of unique
peptides
Pkm
Vim
Pkm
Atp5f1a
Lmna
Lmnb1
Eno1
Atp5f1b
Tkt
Tuba1b
Actb
H1-2
Dlat
Hspa5
Tubb4b
Zyx

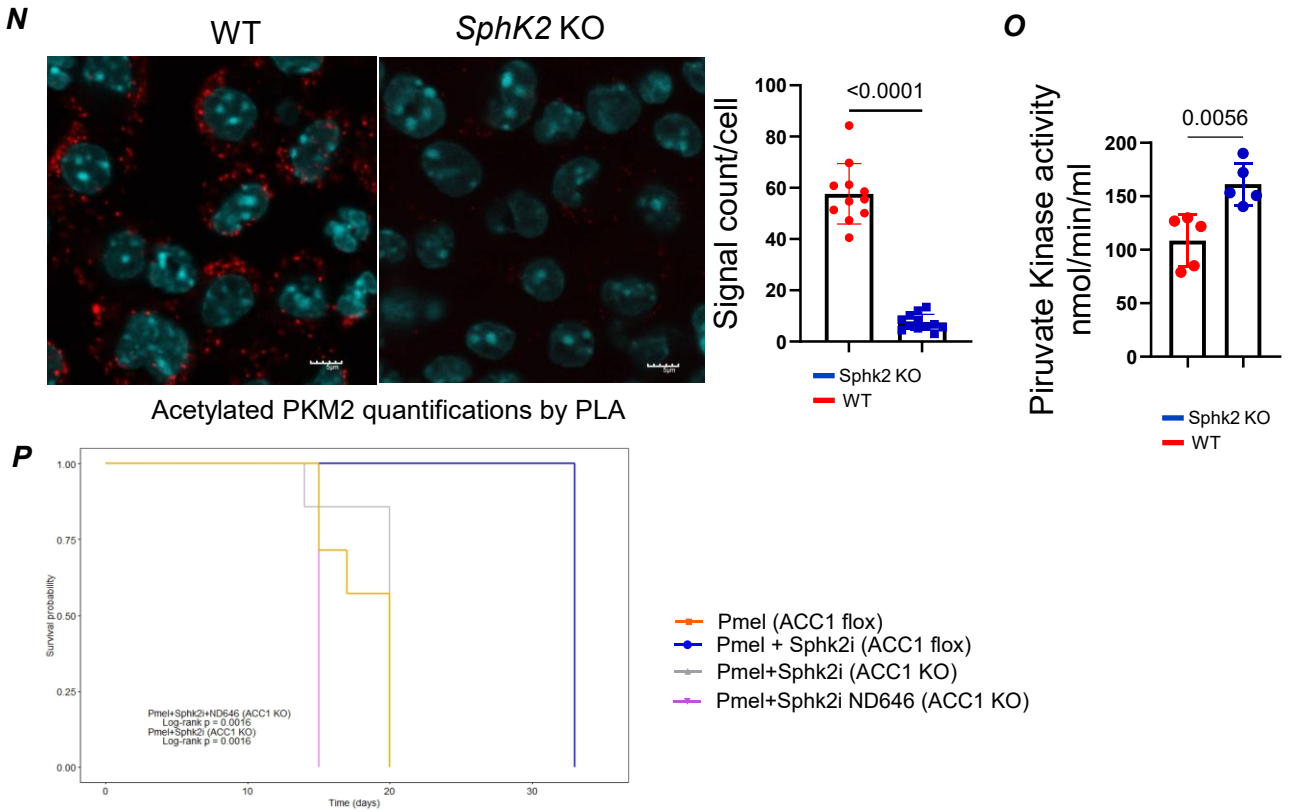

Supplementary Figure 5: A) Bone marrow-derived MDSCs from *SphK2*-KO mice were generated, treated with the indicated doses of ACC inhibitor ND646, and ACC activity was measured. ***B)*** Bone marrow cells from WT and *SphK2*-KO mice were cultured with GM-CSF (20 ng/mL) and 30% B16-F10 tumor explant supernatant (TES) for four days. Flow cytometry analysis was performed to evaluate the expression of the indicated markers in MDSCs, with and without treatment with the ACC inhibitor ND646 (3 μM). MDSCs were electroporated with ACC1, ACC2, or scrambled negative control siRNA and cultured in the same media for two additional days. On day four, MDSCs were analyzed for *ACC1* ***(C)***, *ACC2* ***(D)*** expression using qPCR, and total ACC activity ***(E). F)*** Gating strategy used to identify $Ly6C^{high}$ $Ly6G^{low}$ M-MDSCs generated in Fig 5A and (B, this figure) and analyzed for the indicated markers by flow cytometry ***(G)***. Cells from (*B*) were incubated with gp100 Ag for 16 hours, washed, and co-cultured with CTV-labelled $CD8^+$ Pmel T cells for three days. Gating strategy used to identify $CD8^+$ T cells ***(H)***. T Cell proliferation was evaluated in CD8+ T cells by flow cytometric analysis (***I***). n = 5 biologically independent replicates.

J) MDSCs were generated as described in (*C*) and the indicated groups were analyzed *via* LC-MS for untargeted lipidomic profiling. Principal component analysis (PCA) revealed distinct lipidomic signatures between different groups. The heatmap displays significantly different lipid species across samples (***K***). n = 4 mice/group. ***L)*** EL-4 tumor was established in C57BL/6 mice for two weeks, $Gr1^+CD11b^+$ MDSCs were isolated, and the abundance of PC was measured using a kit following the manufacturer's protocol.

M) Bone marrow cells from WT and *SphK2*-KO mice were cultured with GM-CSF at 20 ng/mL and 30% B16-F10 tumor explant supernatant for four days. Acetylated proteins were pulled down using a total acetylated antibody and analyzed by mass spectrometry. Scatter plot showing the total number of unique peptides detected for the indicated proteins in the proteomic dataset. PKM (pyruvate kinase M) exhibited one of the highest peptide counts (indicated by red arrow), indicating strong representation in the dataset. ***N)*** MDSCs derived from WT and SphK2 KO were used to detect PKM2 acetylation using rabbit anti-mouse PKM-2 and mouse anti-acetyl-lysine by PLA. ***O)*** The cells used in (*N*) were used to determine the pyruvate kinase activity using a commercially available kit as per the manufacturer's protocol. (n = 3 mice/ group).

P) B16-F10 tumors were established in $Acc1^{fl/fl}$ or $LysM^{cre}$ $Acc1^{fl/fl}$ mice as indicated (n = 7 mice/group). Pmel T cells were transferred on day 9 after tumor implantation, and mice received ND646 (25 mg/kg) and/or *SphK2i* (50 mg/kg) as indicated. Kaplan–Meier survival analysis is shown.

Data is presented as mean ± SD. Statistical significance was determined using an unpaired two-tailed Student's t test for comparisons between two groups and one-way ANOVA with Šídák's multiple comparisons test for multiple group comparisons.

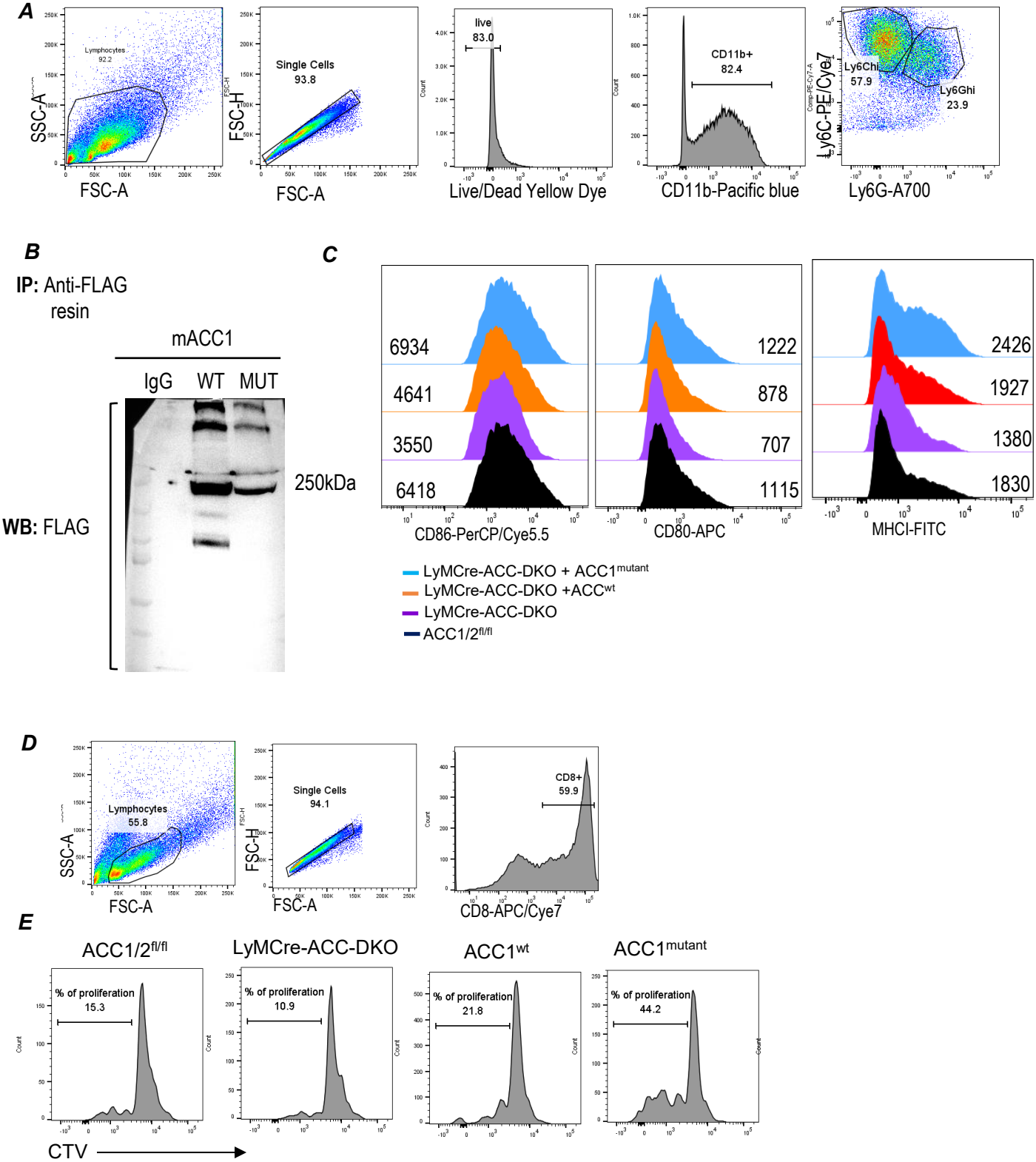

Supplementary Figure 6: A) Bone marrow cells from ACC1/2$^{fl/fl}$, LyM^{Cre}ACC-DKO mice were cultured in the presence of GM-CSF and B16-F10 melanoma tumor explant. MDSCs were then overexpressed with WT or mutated *ACC1* plasmids. Cells were analyzed for the indicated cell surface markers using flow cytometry. Gating strategy used to identify Ly6C^{high} Ly6G^{low} M-MDSCs in bone marrow-derived MDSCs. ***B)*** HEK293T cells were transfected with the FLAG-tagged ACC1^{WT} or ACC1^{mutant} plasmid. Cell lysates were subjected to FLAG immunoprecipitation using agarose-conjugated anti-FLAG antibodies. Representative immunoblot showing levels of immunoprecipitated ACC1^{WT} or ACC1^{mutant} proteins used for the binding assays. ***C)*** M-MDSCs from *(A)* were analyzed for the indicated cell surface markers using flow cytometry. ***D)*** Cells from (*A*) were incubated with gp100 peptide antigen for 16 hours, washed, and co-cultured with CTV-labelled CD8^{+} Pmel T cells for three days. Gating strategy used to identify CD8^{+} T cells. T cell proliferation was evaluated in CD8^{+} T cells by flow cytometric analysis ***(E)***.

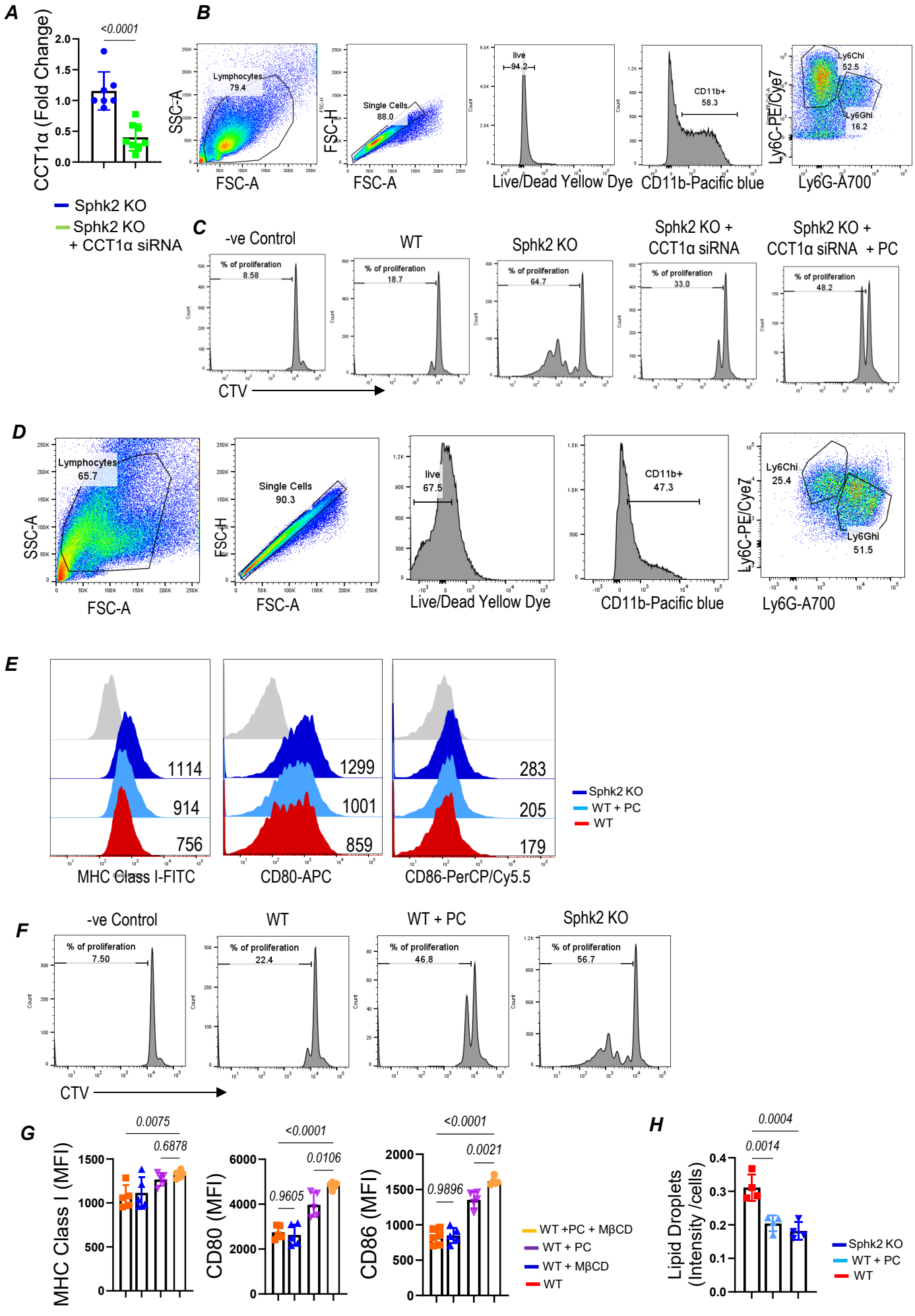
A
CCT1α (Fold Change)
<0.0001
Sphk2 KO
Sphk2 KO + CCT1α siRNA
B
Lymphocytes 79.4
SSC-A
FSC-A
Single Cells 88.0
FSC-H
live 94.2
Live/Dead Yellow Dye
CD11b+ 58.3
CD11b-Pacific blue
Ly6Chi 52.5
Ly6Ghi 16.2
Ly6C-PE/Cye7
Ly6G-A700
C
-ve Control
WT
Sphk2 KO
Sphk2 KO + CCT1α siRNA
Sphk2 KO + CCT1α siRNA + PC
% of proliferation 8.58
% of proliferation 18.7
% of proliferation 64.7
% of proliferation 33.0
% of proliferation 48.2
CTV
D
Lymphocytes 65.7
Single Cells 90.3
live 67.5
CD11b+ 47.3
Ly6Chi 25.4
Ly6Ghi 51.5
E
1114
914
756
1299
1001
859
283
205
179
MHC Class I-FITC
CD80-APC
CD86-PerCP/Cy5.5
Sphk2 KO
WT + PC
WT
F
-ve Control
WT
WT + PC
Sphk2 KO
% of proliferation 7.50
% of proliferation 22.4
% of proliferation 46.8
% of proliferation 56.7
CTV
G
MHC Class I (MFI)
0.0075
0.6878
CD80 (MFI)
<0.0001
0.9605
0.0106
CD86 (MFI)
<0.0001
0.9896
0.0021
WT +PC + MβCD
WT + PC
WT + MβCD
WT
H
Lipid Droplets (Intensity /cells)
0.0004
0.0014
Sphk2 KO
WT + PC
WT

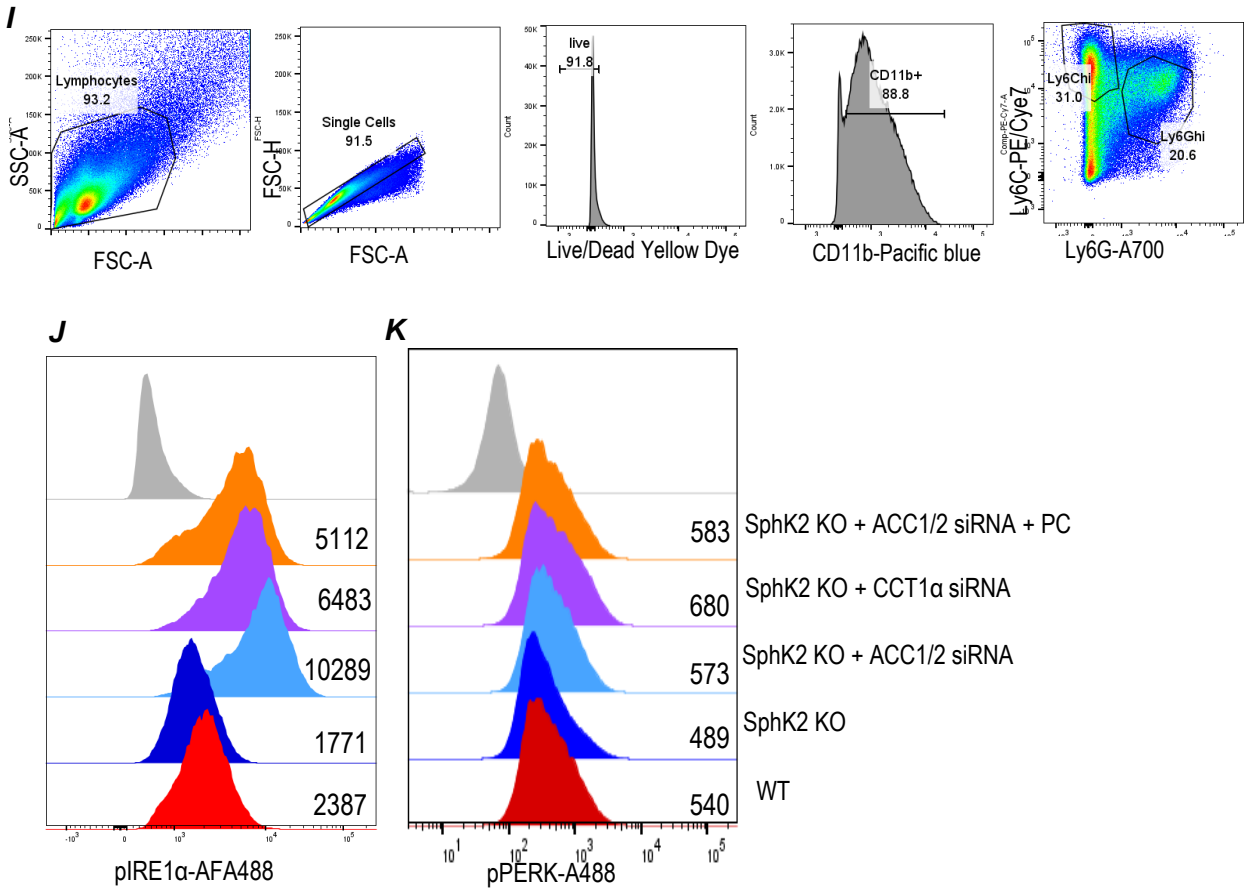

Supplementary Figure 7: A) Bone marrow cells from *SphK2*-KO mice were electroporated with *CCT1α* or scrambled negative control siRNA and were analyzed for *CCT1α* expression using qPCR and Gating strategy used to identify Ly6C^{high} Ly6G^{low} M-MDSCs ***(B)***. ***C)*** Cells from *(A)* were cultured in the same media in the presence or absence of BSA-conjugated PC (30 μM) for two additional days. Cells were then incubated with gp100 peptide antigen for 16 hours, washed, and co-cultured with CTV-labelled CD8^{+} Pmel T cells for three days. T cell proliferation was evaluated in CD8^{+} T cells. **D*)*** EL-4 tumor was established in WT and *SphK2* KO mice for two weeks. M-MDSCs were isolated from the ascitic tumor site and cultured in the presence or absence of PC derived from Soya (30 μM) and gating strategy to identify M-MDSCs. ***E)*** M-MDSCs from *(D)* were analyzed for the indicated markers using flow cytometry. ***F)*** M-MDSCs from *(D)* were incubated with gp100 peptide antigen for 16 hours, washed, and co-cultured with CTV-labelled CD8^{+} Pmel T cells for three days. T Cell proliferation was evaluated in CD8^{+} T cells by flow cytometric analysis. ***G)*** Bone marrow cells from WT mice were cultured with GM-CSF (20 ng/mL) and 30% B16-F10 tumor explant supernatant (TES) for 4 days to generate MDSCs. On day 2, indicated groups were treated with 5 μM MβCD in serum-free media for 1 h at 37 °C. Cells were then washed extensively with warm PBS and cultured for an additional 48 hrs. in the same media supplemented with 30 μM soy PC complexed with fatty acid–free BSA. M-MDSCs from the indicated groups were analyzed for the specified markers by flow cytometry. ***H)*** Bone marrow-derived WT and *SphK2*-KO MDSCs were incubated overnight with BSA-conjugated oleic acid (100 μM) in the presence or absence of BSA-conjugated PC (30 μM). LDs were stained with BODIPY (green) and nuclei counterstained with Hoechst (blue) and imaged. Quantification of LD intensity normalized to cell number. (***I)*** Bone marrow-derived MDSCs were electroporated with *ACC1, ACC2, CCT1α*, or scrambled negative control siRNA and cultured in the same media for two additional days. BSA-conjugated PC (30 μM) was added to the media in the indicated group. Gating strategy used to identify Ly6C^{high} Ly6G^{low} M-MDSCs in bone marrow-derived MDSCs. pITE1α ***(J)*** and pPERK ***(K)*** expression were checked using flow cytometry in M-MDSCs.

Data is presented as mean ± SD of n = 5 independent experiments unless otherwise specified. Statistical significance was determined using an unpaired two-tailed Student's t test for comparisons between two groups and one-way ANOVA with Šídák's multiple comparisons test for multiple group comparisons.

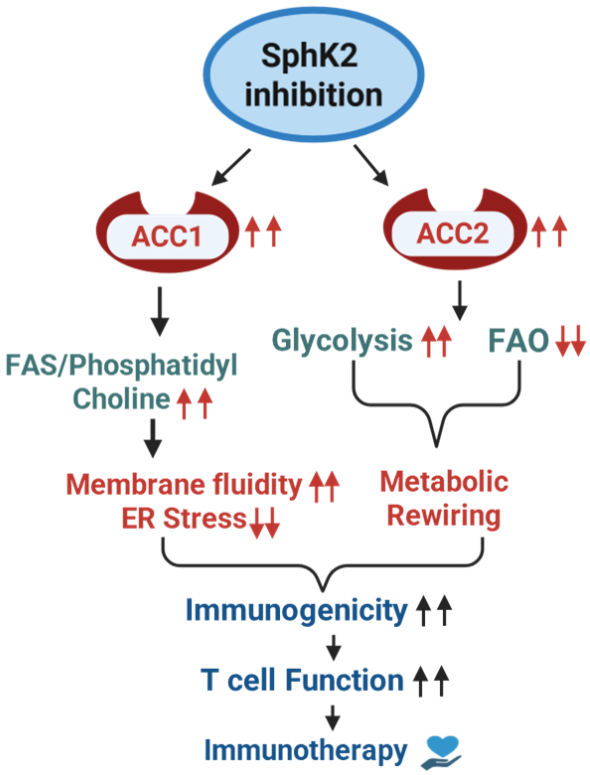

Supplementary Figure 8: *SphK2 inhibition promotes ACC-driven lipid reprogramming to enhance MDSC immunogenicity (Created in BioRender. MEHROTRA, S. (2026) https: l/BioRender.coml i20a424).*

- S1P directly binds to acetyl-CoA carboxylase (ACC) and inhibits its enzymatic activity in monocytic MDSCs (M-MDSCs).
- SphK2 inhibition reduces S1P levels, thereby restoring ACC activity.
- Enhanced ACC activity promotes phosphatidylcholine synthesis and metabolic rewiring.
- Lipid remodeling drives immunogenic differentiation of MDSCs, enhancing T cell function and responses to immunotherapy.

Supplementary Table 1 (Key Resource Table)

REAGENT or RESOURCE	SOURCE	IDENTIFIER
Antibodies		
Anti-mouse CD3	BioXCell	Clone: 145-2C11; Cat# BE0001-1; RRID: AB_1107634
Anti-mouse CD28	BioXCell	Clone: 37.51; Cat# BE0015-1; RRID: AB_1107624
Anti-mouse Ly6G/Ly6C (Gr-1)	BioXCell	Clone: RB6-8C5; Cat# BE0075; RRID: AB_1107721
Anti-mouse CSF1R (CD115)	BioXcell	Clone: AFS98; Cat# BE0213; RRID: AB_2687699
CD4-PE	eBioscience	Clone: GK5.1; Cat# 12-0041-83; RRID: AB_465506
CD4-PE/Cy7	Biolegend	Clone: GK5.1; Cat# 100422; RRID: AB_312707
Arginase 1-APC	eBioscience	Clone: A1exF5; Cat# 17-3697-82; RRID: AB_2572560
Arginase 1-PE/Cy7	eBioscience	Clone: A1exF5; Cat# 25-3697-82; RRID: AB_2573453
CD4-APC/Cy7	Biolegend	Clone: GK5.1; Cat# 100414; RRID: AB_312699
CD8-APC/Cy7	Biolegend	Clone: 53-6.7; Cat# 100714; RRID: RRID: AB_312753
Anti-human HLA-DR APC/Cyanine7	Biolegend	Clone: L243; Cat# 307617; RRID: AB_493586
Anti-human CD33-AF-700	Biolegend	Clone: WM53; Cat# 303435; RRID: AB_2562139
Anti-human CD3-AF-700	Biolegend	Clone: OKT3; Cat# 317340; RRID: AB_2562124
Anti-human CD14 PerCP/Cyanine5.5	Biolegend	Clone: QA18A22; Cat# 398711; RRID: AB_571930
Anti-human CD80 PerCP/Cyanine5.5	Biolegend	Clone: 2D10; Cat# 305231; RRID: AB_2563467
Anti-human CD80 PerCP/Cyanine5.5	Biolegend	Clone: 2D10; Cat# 305231; RRID: AB_314502
Anti-human CD86 PE/Cyanine7	Biolegend	Clone: IT2.2; Cat# 305231; RRID: AB_314539
Anti-human CD15 (SSEA-1)-PE	Biolegend	Clone: W6D3; Cat# 980506; RRID: AB_2572065
Anti-human CD66b-Pacific Blue	Biolegend	Clone: G10F5; Cat# 305111; RRID: AB_2562622
CD80-APC	Biolegend	Clone: 16-10A1; Cat# 104714; RRID: AB_313699
F4/80-FITC	Biolegend	Clone: BM8; Cat# 123110; RRID: AB_893480

F4/80-BV785	Biolegend	Clone: BM8; Cat# 123141; RRID: AB_2564219
I-A/I-E-APC/Cyanine7	Biolegend	Clone: M5/114.15.2; Cat# 107627; RRID: AB_493727
H-2Kb-FITC	BD Pharmingen	Clone: AF6-88.5; Cat# 553569; RRID: AB_394927
CD86 PerCP/Cyanine5.5	Biolegend	Clone: GL-1; Cat# 105028; RRID: AB_493726
CD80 (APC)	Biolegend	Clone: 16-10A1; Cat# 104713; RRID: AB_961406
Ly-6G/Ly-6C (Gr-1) APC/Cyanine7	Biolegend	Clone: RB6-8C5; Cat# 108423; RRID: AB_893561
CD11b-Pacific blue	Biolegend	Clone: M1/70; Cat# 101224; RRID: AB_389305
CD163-APC	Biolegend	Clone: S15049F: Cat# 156705; RRID: AB_313496
CD45.1-PE	Biolegend	Clone: A20; Cat# 110707; RRID: AB_313496
CD45.1-APC/Cyanine7	Biolegend	Clone: A20; Cat# 110715; RRID: AB_313505
CD45.2-AF700	Biolegend	Clone: 104; Cat# 109822; RRID: AB_493735
CD45.2-PE/Cyanine7	Biolegend	Clone: 104; Cat# 109830; RRID: AB_1186098
IL-12/IL-23 p40-APC	Biolegend	Clone: C15.6; Cat# 505205; RRID: AB_315454
IFNγ-Alexa647	Biolegend	Clone: XMG1.2; Cat# 505814; RRID: AB_493314
CD44-PerCP/Cy5.5	Biolegend	Clone: IM7; Cat# 103032; RRID: AB_2076204
IL10-APC	Biolegend	Clone: JES5-16E3; Cat# 505010; RRID: AB_315349
PD-1-PE/Cyanine7	Biolegend	Clone: RMP1-30; Cat# 109110; RRID: AB_572017
LAG-3-PerCP/Cyanine5.5	Biolegend	Clone: C9B7W; Cat# 125212; RRID: AB_10639946
CD33-APC	Biolegend	Clone: P67.6; Cat# 303408; RRID: AB_314357
Vβ13-FITC	BD Biosciences	Clone: MR1 2-3; Cat# 553204; RRID: AB_394706
Ly-6C-PE/Cyanine7	Biolegend	Clone: HK1.4; Cat# 128018; RRID: AB_1732086
Phospho-IRE1α (S724)	Thermo Fisher Scientific	Clone: Polyclonal; Cat# PA1-16927; RRID: AB_2172559
Ly-6G-AF700	Biolegend	Clone: 1A8; Cat# 127622; RRID: AB_10612739

CD163-APC	Biolegend	Clone: S15049I; Cat# 155305; RRID: AB_2814059
Anti-rabbit Alexa Fluor 488	Abcam	Cat# ab150077; RRID: AB_2630356
Phospho-PERK (Thr980)	Cell Signaling Technology	Clone: 16F8; Cat# 3179; RRID: AB_2095847
SPHK2 Polyclonal Antibody	Thermo Fisher Scientific	Cat# 17096-1-AP; RRID: AB_2198897
SPHK2 Polyclonal Antibody	Bioss Antibodies	Cat# bs-2653R; RRID: AB_10856265
Anti-CD11b antibody [EPR1344]	Abcam	Cat# ab133357; RRID: AB_11154537
Mouse qPCR primers: Oligonucleotide Sequences (5′−3′)		
Acaca Forward GTTCTGTTGGACAACGCCTTCAC	This Paper	N/A
Acaca Reverse GGAGTCACAGAAGCAGCCCATT	This Paper	N/A
Acacb Forward AGAAGCGAGCACTGCAAGGTTG	This Paper	N/A
Acacb Reverse GGAAGATGGACTCCACCTGGTT	This Paper	N/A
Pcyt1a Forward TCCTTCCAAAGTGCAGCGTTGC	This Paper	N/A
Pcyt1a Reverse GCAGGCTTCTTCCATAGTCACC	This Paper	N/A
Mouse SiRNA		
Pcyt1a	Ambion (Thermo Fisher Scientific)	Cat# AM16708, ID# 161380
Acaca	Ambion (Thermo Fisher Scientific)	Cat# 4390771, ID# s98861
Acacb	Ambion (Thermo Fisher Scientific)	Cat# 4390771, ID# s97643
Chemicals, Peptides, and Recombinant Proteins, Critical Commercial Assays		
L-alpha-Phosphatidylcholine, solution, from soybean, Type III-S	Sigma-Aldrich	Cat# P3782
Fatty acid-free BSA	Sigma-Aldrich	Cat# A8806
ND-646	MedChemExpress	Cat# HY-101842
Biotin	Cayman Chemical	Cat# 22582
Sphingosine (d17:1)	Cayman Chemical	Cat# 10007902
S1P-biotin	Echelon Biosciences	Cat# S-200B
S1P	Echelon Biosciences	Cat# S-2000
Methyl-β-cyclodextrin	Sigma-Aldrich	Cat# C4555
LIVE/DEAD Fixable Yellow Dead Cell Stain Kit	Thermo Fisher Scientific	Cat# L34959

T cell negative selection kits (MagniSort)	Invitrogen	Cat # 8804-6820-74
Myeloid-Derived Suppressor Cell Isolation Kit (mouse)	Miltenyi Biotech	Cat# 130-094-538)
Acetyl CoA Carboxylase Assay Kit	MyBioscouse	Cat# MBS8303295
Pyruvate Kinase Activity Assay Kit	Abcam	Cat# ab83432
Phosphatidylcholine Assay Kit	Sigma-Aldrich	Cat# MAK049
Biotin ELISA Kit	CD Creative Diagnostics	Cat# DEIA9990
Signal-Seeker Acetyl-Lysine Detection Kit	Cytoskeleton	BK163-S
Membrane fluidity kit	Abcam	Cat# ab189819
Lipofectamine 3000 Transfection Reagent	Thermo Fisher Scientific	Cat# L3000008
Mouse T Cell Nucleofector Kit	Lonza	Cat# VPA-1006
Mouse Tumor Dissociation Kit	Miltenyi Biotec	Cat# 130-096-730
2-Deoxy-D-glucose (2DG)	Sigma Aldrich	Cat# D6134
Antimycin A	Sigma Aldrich	Cat# A8674
Rotenone	Sigma Aldrich	Cat# R8875
Oligomycin	Sigma Aldrich	Cat# O4876
FCCP	Sigma Aldrich	Cat# C2920
BSA-Oleate Monounsaturated Fatty Acid Complex	Cayman Chemicals	Cat# 29557
BODIPY 493/503	Thermo Fisher Scientific	Cat# D3922
IMDM	GE Healthcare, HyClone	Cat# SH30228.01
RPMI-1640 (methionine free)	Thermo Fisher Scientific	Cat# A1451701
Penicillin-Streptomycin	Corning	Cat# 30-001-CI
Fetal Bovine Serum (FBS)	Atlanta Biologicals	Cat# S11150
rGM-CSF	Biolegend	Cat# 576302
G-CSF	Biolegend	Cat# 574604
rhIL2	NCI, Biological Resources Branch	https://ncifrederick.cancer.gov/research/brb/productDataSheets/cytokineHumanInterleukins/IL-2Bulk.aspx
Foxp3 / Transcription Factor Staining Buffer Set	Thermo Fisher Scientific	Cat# 00-5523
Fixation/Permeabilization Solution Kit	BD Biosciences	Cat# 554714
hgp100$_{25-33}$ peptide (KVPRNQDW)	Genscript	Cat# RP20344
RIPA Lysis Buffer	Thermo Fisher Scientific	Cat# 89900
Cell Trace Violet Cell Proliferation Kit	Thermo Fisher Scientific	Cat# C34557
iScript cDNA Synthesis Kit	Biorad	Cat# 1708891
SsoAdvanced Universal SYBR Green Supermix	Biorad	Cat# 1725274
Experimental Models: Cell Lines		
B16-F10	ATCC	CRL-6475
EL4	ATCC	TIB-39

4T1	ATCC	CRL-2539
Experimental Models: Organisms/Strains		
C57BL/6	Jackson Laboratory	Stock# 000664
B6.SJL-Ptprca Pepcb/BoyJ (B6 CD45.1)	Jackson Laboratory	Strain #:033076
Acacatm1Jdh/J (Acc1 flox)	Jackson Laboratory	Strain #:030954
D2.129P2(B6)-Lyz2tm1(cre)Ifo/SjJ (LysMCre)	Jackson Laboratory	Strain #:026861
B6N.129S6-Sphk1tm1Rlp/J (SphK1 KO)	Ogretmen's Laboratory	Strain # 019095
B6N.129S6-Sphk2tm1Rlp/J (SphK2 KO)	Ogretmen's Laboratory	Strain # 019140
BALB/cJ	Jackson Laboratory	Strain #:000651
B6.129S7-*Rag1*^{tm1Mom}/J	Jackson Laboratory	Stock# 002216
Software and Algorithms		
FlowJo 10.2	TreeStar, OR	https://www.flowjo.com/solutions/flowjo/downloads/
Prism 9	GraphPad	https://www.graphpad.com/scientific-software/prism/
Agilent Seahorse Wave 2.4	Agilent	http://www.agilent.com/en-us/products/cell-analysis-(seahorse)/seahorse-wave-software
CFX Manager 3.1	Biorad	http://www.bio-rad.com/en-us/sku/soft-cfx-31-patch-cfx-manager-software-v3-1-upgrade